

# ENTROPIC TRANSFER OPERATORS

OLIVER JUNGE<sup>1</sup>, DANIEL MATTHES<sup>1</sup> AND BERNHARD SCHMITZER<sup>2</sup>

ABSTRACT. We propose a new concept for the regularization and discretization of transfer operators in dynamical systems. Our approach is based on the entropically regularized optimal transport between two probability measures. In particular, we use optimal transport plans in order to construct a finite-dimensional approximation of some transfer operator which can be analysed computationally. We prove that the spectrum of the discretized operator converges to the one of the regularized original operator, give a detailed analysis of the relation between the discretized and the original peripheral spectrum for a rotation map on the  $n$ -torus and provide code for three numerical experiments, including one based on the raw trajectory data of a small biomolecule from which its dominant conformations are recovered.

## 1. INTRODUCTION

1.1. **Motivation.** We propose a novel approach to the following problem from dynamical systems: *Given a deterministic map  $F : \mathcal{X} \rightarrow \mathcal{X}$  on a large (continuous and possibly high-dimensional) state space  $\mathcal{X}$ , find a stochastic (i.e. distribution-valued) map  $F^N$  on a small (i.e. finite) state space  $\mathcal{X}^N \subset \mathcal{X}$  that “captures the most relevant features” of  $F$ .* Here,  $N \in \mathbb{N}$  denotes a discretization scale and we will often be interested in the limit  $N \rightarrow \infty$ . Our idea for the construction of  $F^N$  is to smooth the action of the deterministic map  $F$  on  $\mathcal{X}^N$  by means of an entropically regularized optimal transport plan.

Concerning the stochastic formulation, we shall assume that  $F$  possesses some interesting invariant probability measure  $\mu$  (i.e. a natural resp. SRB-measure) and consider the stochastic formulation of  $F$ 's deterministic dynamics via the transfer operator  $T : L^2(\mu) \rightarrow L^2(\mu)$  given by  $Th := d[F_{\#}(h\mu)]/d\mu$  (where  $F_{\#}\nu$  denotes the push-forward of the measure  $\nu$  under  $F$ ). Intuitively, if points are distributed according to  $h\mu$  on  $\mathcal{X}$ , then their images are distributed according to  $(Th)\mu$ . Since  $F$  is deterministic,  $T$  is an  $L^2$ -isometry. We then define  $F^N$  via a transfer operator  $T^{N,\varepsilon} : L^2(\mu^N) \rightarrow L^2(\mu^N)$ , where  $\mu^N$  is an approximate invariant probability measure for the stochastic dynamics, and  $\varepsilon$  denotes the magnitude of regularization.

---

<sup>1</sup>DEPARTMENT OF MATHEMATICS, TECHNICAL UNIVERSITY OF MUNICH, GERMANY

<sup>2</sup>INSTITUTE OF COMPUTER SCIENCE, UNIVERSITY OF GÖTTINGEN, GERMANY

*E-mail addresses:* oj@tum.de, matthes@ma.tum.de, schmitzer@cs.uni-goettingen.de.

*Date:* April 12, 2022.

This research was supported by the DFG Collaborative Research Center TRR 109, “Discretization in Geometry and Dynamics”. BS was supported by the Emmy Noether Programme of the DFG (project number 403056140).

A similar regularization can be applied to  $T$  itself, yielding the operator  $T^\varepsilon : L^2(\mu) \rightarrow L^2(\mu)$ . Informally, compared to  $T$ , the regularized operator  $T^\varepsilon$  smooths spatial structures below the length scale  $\sqrt{\varepsilon}$ . We will show that (a suitable extension of)  $T^{N,\varepsilon}$  converges to  $T^\varepsilon$  in operator norm when  $\mu^N \xrightarrow{*} \mu$  as  $N \rightarrow \infty$  for fixed  $\varepsilon > 0$ . That is, for sufficiently high  $N$ , the analysis of  $T^{N,\varepsilon}$  can reveal structural properties of the dynamics of  $F$  above the length scale  $\sqrt{\varepsilon}$ .

Note that it is not our main concern to find a particularly good approximation  $\mu^N$  of  $\mu$ . In examples we demonstrate that simple approximations such as discrete samples from a trajectory can be sufficient. Unlike  $T$ , the genuinely stochastic transfer operators  $T^{N,\varepsilon}$  and  $T^\varepsilon$  are typically not isometries anymore.

Concerning the “most relevant features”, we shall adopt the point of view that these are determined by the peripheral spectrum of  $T^\varepsilon$ . For example, if  $F$  exhibits an (almost)  $n$ -cycle, then this will be represented in the spectrum of  $T^\varepsilon$  by an  $n$ -tuple of eigenvalues close to  $\lambda_k = e^{2\pi ik/n}$ . Similarly, if  $F$  shows metastable behaviour, i.e. the state space  $\mathcal{X}$  decomposes into  $k$  almost invariant sets, the spectrum of  $T^\varepsilon$  contains  $k$  real eigenvalues close to 1.

**1.2. Related work.** A classical approach based on coarse graining is known as Ulam’s method [27], see [14, 10] for modern versions. The original phase space  $\mathcal{X}$  (which might be just the support of the invariant measure  $\mu$ ) is covered by essentially disjoint subsets  $C_i$ . Here,  $F^N$  ( $N$  is the number of subsets) is chosen to reflect the transfer of mass between subsets under the deterministic map  $F$ : that is, if one thinks of  $F^N$  as a stochastic matrix with entry  $(i, j)$  giving the conditional probability of jumping from subset  $j$  to subset  $i$ , then the corresponding value is  $m(C_j \cap F^{-1}(C_i))/m(C_j)$ , where  $m$  denotes the volume measure. Naturally, one hopes that this correspondence between  $F^N$  and the transfer of mass is preserved to good accuracy even after iterations: that is, the  $(i, j)$ -entry of  $(F^N)^n$  should be a reasonably good approximation of  $m(C_j \cap F^{-n}(C_i))/m(C_j)$ . In practice, this correspondence breaks down the sooner the larger the subsets are. In particular, the method requires to calculate the volume of intersections of subsets with preimages of other subsets. This task typically requires that  $F$  can be evaluated at arbitrary points in phase space and quickly becomes infeasible as the dimension of phase space (or the underlying invariant set) increases.

This Markov matrix as an approximation to the transfer operator can be interpreted as a Galerkin discretization of the operator using a dictionary of characteristic functions on the covering [10]. Recently, methods have been proposed which use a different dictionary (often of ansatz functions with global support) and approximate the required space integrals by a fixed set of quadrature points, like (*Kernel-based, extended*) *dynamic mode composition* [30, 31, 17]<sup>1</sup>. These schemes have rapidly gained popularity since they can be applied to problems on high dimensional phase spaces and to problems where only measurement data is available.

---

<sup>1</sup>In these works, the adjoint of the transfer operator, the Koopman operator, is considered. As shown in [17], similar constructions can be made for the transfer operator.

**1.3. Optimal transport.** Similar to Ulam’s method, our approach defines a stochastic map on a discrete set. Stochasticity will be introduced by entropic optimal transport. Optimal transport is a geometrically intuitive and robust notion to compare probability measures by rearranging their mass into each other [28, 25] with applications in a broad range of mathematics. In particular its entropy regularized variant is rather popular in data analysis and machine learning applications [24]. It was recently proposed for the detection of coherent sets from data [18].

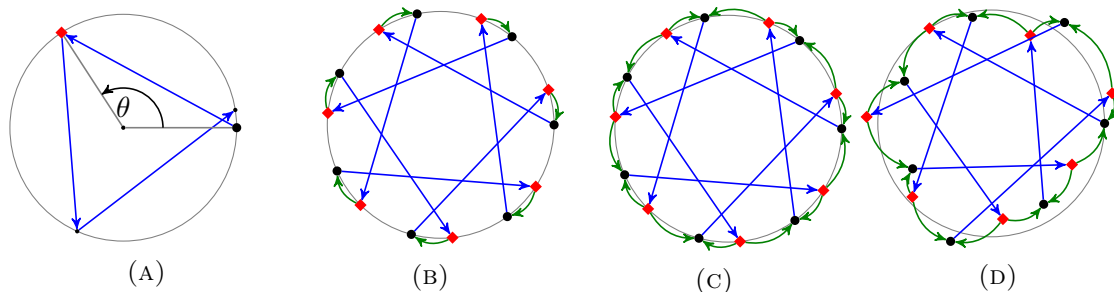


FIGURE 1. (A) The unit circle  $\mathcal{X} = S^1$  with the shift map  $F : \varphi \mapsto \varphi + \theta$  (blue) with  $\theta \approx 2\pi/3$  is a simple dynamical system with an approximate 3-cycle. (B) A naive discretization  $\mathcal{X}^N$  with 7 equidistant points (black circles) poses several problems.  $\mathcal{X}^N$  is not closed under  $F$  and a concatenation of  $F$  (blue) with a deterministic identification (green) of points in  $F(\mathcal{X}^N)$  (red diamonds) with  $\mathcal{X}^N$  yields a single cycle of length 7 that does not reflect the approximate 3-cycle. (C) We show that stochastic identification based on entropic optimal transport with regularization strength  $\epsilon$  (green) provides a consistent way of inferring information about  $F$  as  $N \rightarrow \infty$  on length scales above  $\sqrt{\epsilon}$ . (D) This result also holds when the  $\mathcal{X}^N$  do not exactly lie on the attractor and when they are distributed at random, which provides flexibility on how to obtain  $\mathcal{X}^N$  in practice.

**1.4. Overview and outline.** As in Ulam’s method, the approach presented here approximates the deterministic map  $F$  on  $\mathcal{X}$  by a stochastic model on a discrete set  $\mathcal{X}^N$ , where in our case  $\mathcal{X}^N \subset \mathcal{X}$  is typically a finite collection of points. By continuity of the map  $F$ , it is reasonable to expect that macroscopic features are still observed by “probing” the dynamics only in  $\mathcal{X}^N$  (if this set covers  $\mathcal{X}$  sufficiently well).

However, it makes little sense to simply consider the deterministic map  $F$  restricted to  $\mathcal{X}^N$  since  $\mathcal{X}^N$  is usually not closed under  $F$ , and – even if it were, or if a deterministic identification of points in  $F(\mathcal{X}^N)$  and  $\mathcal{X}^N$  were given – the resulting dynamics is often dominated by combinatorial discretization artifacts (see Figure 1 for an illustration and Section 5.4 for discussion). Instead, we propose a stochastic identification of  $F(\mathcal{X}^N)$  and  $\mathcal{X}^N$  by means of an optimal transport plan with entropic regularization of strength  $\epsilon > 0$  between the uniform distributions of  $F(\mathcal{X}^N)$  and  $\mathcal{X}^N$ . Under this plan the masses of the

image points in  $F(\mathcal{X}^N)$  are distributed such that each point in  $\mathcal{X}^N$  receives precisely a unit amount of mass. The optimal entropic transport plan reflects spatial proximity, i.e., the mass of a point in  $F(\mathcal{X}^N)$  goes preferably to points in  $\mathcal{X}^N$  that are nearby, but it also introduces some stochastic blur on a length scale that depends on the regularization parameter  $\varepsilon$ .

Our approximation of the transfer operator thus uses two elements: the first, conceptual one is the reduction to a dynamics on a subsystem; the second one is a regularization of the pure transfer by a diffuse one. Entropic regularization provides four attractive properties. First, the regularized transport problems can efficiently be solved numerically via the Sinkhorn algorithm. Second, the introduced blur removes discretization artifacts of the deterministic assignment that easily mask the actual macroscopic structure of the dynamics. Third, the blur provides compactness of the transfer operator in the limit of infinitely many points and thus provides convergence to a continuous limit operator at the cost of losing fine-scale information. Finally, by tuning the regularization parameter, dynamical features on specific length scales can be selectively studied. These properties make our approach attractive for the numerical study of the macroscopic properties of dynamical systems as we demonstrate on several examples.

As mentioned, in [18] an approach for the detection of coherent sets in non-autonomous systems has been proposed which also uses the concept of optimal transport. There, it is assumed that two measurements of  $\mu$  and  $F_{\#}\mu$  are given,  $F$  is unknown and  $\mu$  is not assumed to be an invariant measure of  $F$ . A map  $F$  (or rather a corresponding transfer operator  $T$ ) is then estimated by the optimal transport between  $\mu$  and  $F_{\#}\mu$ , and approximately coherent sets are subsequently estimated by a clustering algorithm that uses spectral information from the estimated  $T$ . Entropic smoothing provides a simple numerical algorithm, compactness of  $T$  and validity of the clustering step. In contrast, we assume that an approximation  $\mu^N$  of  $\mu$  and the behaviour of  $F$  on  $\mu^N$  are known where now  $\mu$  is assumed to be an invariant measure of  $F$ . We then perform a detailed spectral analysis of the implied transfer operator. Again, entropic smoothing provides a simple numerical algorithm and compactness of the transfer operator, but in addition in our application entropic transport provides a natural way to deal with the fact that  $F_{\#}\mu^N$  does not exactly equal  $\mu^N$ .

We recall basic properties on transfer operators and (entropic) optimal transport in Sections 2 and 3. In Section 4 we introduce the discrete transfer operator  $T^{N,\varepsilon}$  and the smoothed version  $T^\varepsilon$  of the original operator  $T$  and establish the convergence of (an extension of) the former towards the latter. This is of practical relevance since the former can be analyzed by numerical methods. As a proof of concept, in Section 5 we analytically study the application to the shift map on the  $d$ -torus to provide intuition for the interplay of the length scales associated to eigenfunctions of  $T$ , discretization index  $N$ , and entropic regularization  $\varepsilon$ . Several numerical examples are given in Section 6.

**1.5. General hypotheses and notations.** Throughout this manuscript,  $(\mathcal{X}, d)$  is a compact metric space, and  $F : \mathcal{X} \rightarrow \mathcal{X}$  is a continuous map. We shall occasionally assume

that  $\mathcal{X}$  is a compact subset of  $\mathbb{R}^d$ , but only when explicitly mentioned. Unless stated otherwise, the cost function  $c : \mathcal{X} \times \mathcal{X} \rightarrow \mathbb{R}_{\geq 0}$  for optimal transportation is the canonical one,  $c(x, y) = d(x, y)^2$ .

## 2. BACKGROUND ON TRANSFER OPERATORS

**2.1. Push-forward and invariant measures.** Choose some points  $x_1, \dots, x_n \in \mathcal{X}$  independently according to some probability measure  $\mu$  on  $\mathcal{X}$ , i.e. such that the probability  $\mathbf{P}(x_j \in B)$  to find  $x_j$  in some Borel set  $B$  is  $\mu(B)$ . Then

$$\mathbf{P}(F(x_j) \in A) = \mathbf{P}(x_j \in F^{-1}(A)) = \mu(F^{-1}(A)),$$

i.e. the probability to find some image point  $F(x_j)$  in some Borel set  $A$  is  $\mu(F^{-1}(A))^2$ . Phrasing this differently: If some points  $x_1, \dots, x_n$  are distributed according to the probability measure  $\mu$  then their image points  $F(x_1), \dots, F(x_n)$  are distributed according to the probability measure

$$(1) \quad F_{\#}\mu := \mu(F^{-1}(\cdot)),$$

called the *push-forward measure* of  $\mu$  (under  $F$ ). The mapping  $F_{\#} : \mu \mapsto F_{\#}\mu$  defines a linear operator on the space of bounded signed measures, called *transfer operator* (or *Frobenius-Perron operator*). Clearly, if  $\mu$  is a linear combination of point measures at some points  $x_1, \dots, x_n \in \mathcal{X}$ , i.e.  $\mu = \sum_j a_j \delta_{x_j}$ ,  $a_j \in \mathbb{R}$ , then

$$(2) \quad F_{\#}\mu(A) = \sum_j a_j \delta_{x_j}(F^{-1}(A)) = \sum_j a_j \delta_{F(x_j)}(A)$$

for all Borel sets  $A$ , i.e.  $F_{\#}\mu = \sum_j a_j \delta_{F(x_j)}$ . Additionally, from (1) we directly get that

$$(1) \quad F_{\#}\mu \geq 0 \text{ if } \mu \geq 0 \text{ and}$$

$$(2) \quad \int dF_{\#}\mu = \int d\mu,$$

for any non-negative measure  $\mu$ , i.e.  $F_{\#}$  is a *Markov operator*.

A probability measure which is a fixed point of  $F_{\#}$  is called an *invariant measure*. Invariant measures provide information about, e.g., recurrent behaviour of points:

**Theorem 1** (Poincaré). *Let  $\mu$  be an invariant measure for  $F$ . For some Borel set  $A \subset \mathcal{X}$  let  $A_0$  be the subset of points from  $A$  which return infinitely often to  $A$  under iteration with  $F$ . Then  $\mu(A_0) = \mu(A)$ .*

**2.2. Ulam's method.** Invariant measures can be approximated by eigenvectors of some matrix approximation of  $F_{\#}$ . A particularly popular approximation results from *Ulam's method* [27]: Fix a non-negative reference measure  $m$  (e.g. the Lebesgue measure or a measure concentrated on some invariant set  $\mathcal{A} \subset \mathcal{X}$ , e.g. some attractor) and an  $m$ -essentially

---

<sup>2</sup>We denote by  $F^{-1}(A) = \{x \in \mathcal{X} \mid F(x) \in A\}$  the *preimage* of the set  $A \subset \mathcal{X}$

disjoint covering  $A_1, \dots, A_n$  of the support of  $\mu$ . Instead of solving the eigenproblem  $F_{\#}\mu = \mu$  over all non-negative measures and for all measurable sets, we parametrize

$$\mu = \sum_{j=1}^n h_j \frac{m(A_j \cap \cdot)}{m(A_j)} \quad \text{for non-negative coefficients } h_1, \dots, h_n,$$

and only enforce the condition  $F_{\#}\mu = \mu$  on the sets  $A_j$ ,

$$h_j = \mu(A_j) = (F_{\#}\mu)(A_j) = \sum_{k=1}^n P_{jk} \cdot h_k \quad \text{with coefficients } P_{jk} := \frac{m(A_k \cap F^{-1}(A_j))}{m(A_k)},$$

resulting in the discrete eigenproblem  $Ph = h$  on  $\mathbb{R}^{n \times n}$ .  $P$  is a Markov matrix, i.e. its columns sum to 1 and its entries give the (conditional) probability to map from element  $A_k$  into  $A_j$ .

Ulam's method is easily to implement: Typically, one chooses a suitable set of sample points in each  $A_j$  (e.g. on a grid or randomly) and computes the location of their images in order to approximate the transition probabilities  $P_{jk}$  [14, 15]. Convergence (as the number  $n$  of covering sets goes to infinity) is slow [2] since the ansatz is of low regularity. If combined with appropriate numerical methods for computing a covering of some underlying invariant set  $\mathcal{A} \subset \mathcal{X}$  first [9, 10], one can efficiently approximate invariant measures on low-dimensional invariant sets, even if the underlying state space  $\mathcal{X}$  is high dimensional. Typically, however, the numerical effort for constructing the covering scales exponentially in the dimension of the invariant set.

**2.3. Other eigenvalues.** As mentioned, invariant measures are fixed points of  $F_{\#}$ , i.e. eigenmeasures at the eigenvalue 1. But other eigenpairs might also be of interest. Roots of unity reveal (macroscopic) cycling behaviour, while real eigenvalues close to 1 can be used to detect almost invariant sets, i.e. metastable dynamics [10]: Let  $F_{\#}\nu = \lambda\nu$ ,  $\nu = h\mu$ ,  $h \in L^1(\mu)$ , for some real  $\lambda < 1$ ,  $\lambda \approx 1$ , then the sets  $A^- := \{h < 0\}$  and  $A^+ := \{h > 0\}$  have the property that the ‘‘internal’’ transition probability

$$p(A^\pm) := \frac{\nu(A^\pm \cap F^{-1}(A^\pm))}{\nu(A^\pm)}$$

to stay in  $A^-$  resp.  $A^+$  under one iteration of  $F$  is close to 1. We will demonstrate this kind of macroscopic behaviour in the experiments section. This can immediately be applied to other eigenpairs of the matrix  $P$  from Ulam's method. In the general case this spectral analysis may be more convenient on densities, see below.

**2.4. Push-forward for densities.** Sometimes it is more convenient to restrict oneself to measures that are absolutely continuous with respect to some reference measure  $\mu$ . The push-forward under  $F$  induces a linear map  $T : L^1(\mu) \rightarrow L^1(F_{\#}\mu)$  where  $Th$  is characterized by

$$(3) \quad \int_{\mathcal{X}} \varphi(y) (Th)(y) d(F_{\#}\mu)(y) = \int_{\mathcal{X}} \varphi(F(x)) h(x) d\mu(x),$$

for continuous test functions  $\varphi : \mathcal{X} \rightarrow \mathbb{R}$ , or, more colloquially,

$$(4) \quad Th := \frac{d(F_{\#}(h\mu))}{d(F_{\#}\mu)}.$$

If  $F$  is a homeomorphism this simplifies to  $Th = h \circ F^{-1}$  (and becomes essentially independent of  $\mu$ ). For any convex function  $J$  one can show with Jensen's inequality, see [5, Lemma 3.15],

$$(5) \quad \int_{\mathcal{X}} J \circ (Tf) \, d(F_{\#}\mu) \leq \int_{\mathcal{X}} J \circ f \, d\mu,$$

hence  $Th$  indeed lies in  $L^1(F_{\#}\mu)$  and in fact the appropriate restrictions of  $T$  are continuous linear operators from  $L^p(\mu)$  to  $L^p(F_{\#}\mu)$  for any  $p \geq 1$ .

If  $\mu$  happens to be invariant under  $F$ , i.e.,  $F_{\#}\mu = \mu$ , then  $T$  is actually a continuous linear self-mapping on each  $L^p(\mu)$ , and in particular on the Hilbert space  $L^2(\mu)$ . In this case a spectral analysis of  $T$  can reveal the dynamic structure of  $F$ .

The definition above, however, makes sense even if  $\mu$  is not invariant. The necessity to consider transfer operators with respect to non-invariant measures arises e.g. when  $\mu$  is an approximation of a genuinely invariant measure by point masses, in which case  $F_{\#}\mu$  is not only different from  $\mu$ , but typically not even absolutely continuous with respect to  $\mu$ , making spectral analysis impossible. The method we introduce below modifies  $T$  by means of optimal transport in such a way that it is always a self-mapping on  $L^p(\mu)$ , thus making spectral analysis feasible again.

### 3. BACKGROUND ON PLAIN AND ENTROPIC OPTIMAL TRANSPORT

Extensive introductions to optimal transport can be found in [28, 25], computational aspects are treated in [24]. Here we briefly summarize the ingredients required for our method.

**3.1. The original optimal transport problem.** The basic problem in the mathematical theory of optimal transport (OT) is the following: given two mass distributions, represented by probability measures  $\mu, \nu \in \mathcal{P}(\mathcal{X})$ , and a function  $c : \mathcal{X} \times \mathcal{X} \rightarrow \mathbb{R}$  that assigns the cost  $c(x, y)$  to the transfer of one unit of mass from  $x \in \mathcal{X}$  to  $y \in \mathcal{X}$ , find the most cost efficient way to “re-distribute”  $\mu$  into  $\nu$ . The first mathematically sound definition of “re-distribute” was due to Monge [21] in terms of maps  $\Phi : \mathcal{X} \rightarrow \mathcal{X}$  that transport  $\mu$  to  $\nu$ , i.e.

$$(6) \quad \Phi_{\#}\mu = \nu.$$

In that class of transport maps, one seeks to minimize the total cost associated with  $\Phi$ , given by

$$(7) \quad \int_{\mathcal{X}} c(x, \Phi(x)) \, d\mu(x).$$

This formulation is very intuitive, since  $\Phi$  assigns to each original mass position  $x$  a target position  $\Phi(x)$ . But an optimal map  $\Phi$  need not exist in general. A prototypical obstacle is

that if  $\mu$  charges some single point  $x$  with positive mass (which is the situation of interest here), then this mass may need to be split into several parts going to different target points  $y$  charged by  $\nu$ .

**3.2. Kantorovich relaxation and Wasserstein distances.** Additional flexibility is provided by Kantorovich's relaxation. It is formulated with so-called transport plans, which are probability measures  $\gamma \in \mathcal{P}(\mathcal{X} \times \mathcal{X})$  with marginals  $\mu$  and  $\nu$  respectively. We denote the set of transport plans by

$$(8) \quad \Gamma(\mu, \nu) := \left\{ \gamma \in \mathcal{P}(\mathcal{X} \times \mathcal{X}) \mid \pi_{\#}^1 \gamma = \mu, \pi_{\#}^2 \gamma = \nu \right\},$$

where  $\pi^i : \mathcal{X} \times \mathcal{X} \rightarrow \mathcal{X}$  denotes the map  $(x_1, x_2) \mapsto x_i$  for  $i = 1, 2$ . The constraints correspond to the condition (6). For measurable  $A, B \subset \mathcal{X}$ , one interprets  $\gamma(A \times B)$  as the mass that is transported from  $A$  to  $B$ . Accordingly, the minimization problem (7) becomes

$$(9) \quad \mathcal{C}(\mu, \nu) := \inf_{\gamma \in \Gamma(\mu, \nu)} \int_{\mathcal{X} \times \mathcal{X}} c(x, y) \, d\gamma(x, y).$$

Unlike for (7), admissible  $\gamma$  always exist, e.g. the product measure  $\mu \otimes \nu \in \Gamma(\mu, \nu)$ . Existence of an optimal plan  $\gamma_{\text{opt}}$  follows from mild assumptions, e.g. when  $c$  is continuous [28]. For  $\mathcal{X} \subset \mathbb{R}^d$ ,  $c(x, y) = d(x, y)^2 = \|x - y\|^2$ , Brenier's fundamental theorem [4] says that  $\gamma_{\text{opt}}$  is actually not far from being a map. Namely, its support lies in the graph of the subdifferential of a convex function. Efficient numerical solvers for the optimal transport problem all use that sparsity in one way or the other.

In our case  $c(x, y) := d(x, y)^2$  the map  $(\mu, \nu) \mapsto W_2(\mu, \nu) := \sqrt{\mathcal{C}(\mu, \nu)}$  is called the 2-Wasserstein distance which is a metric on  $\mathcal{P}(\mathcal{X})$  that metrizes weak\* convergence. For non-compact metric  $\mathcal{X}$  additional conditions on the moments of  $\mu, \nu$  apply. The construction works equivalently for arbitrary exponents  $p \in [1, \infty)$ .

**3.3. Entropic regularization.** The basic optimal transport problem (9) is convex but not strictly convex. That "flatness" is often an obstacle, both in the analysis and for efficient numerical treatment. A way to overcome it is *entropic regularization*. It amounts to augmenting the variational functional in (9) by a regularizing term:

$$(10) \quad \mathcal{C}^\varepsilon(\mu, \nu) := \inf_{\gamma \in \Gamma(\mu, \nu)} \int_{\mathcal{X} \times \mathcal{X}} c(x, y) \, d\gamma(x, y) + \varepsilon \mathbf{H}(\gamma \mid \theta),$$

where  $\mathbf{H}(\cdot \mid \theta)$  is the probabilistic entropy with respect to some non-negative reference measure  $\theta$  on  $\mathcal{X} \times \mathcal{X}$ ,

$$\mathbf{H}(\gamma \mid \theta) := \int_{\mathcal{X} \times \mathcal{X}} \left( \log \frac{d\gamma}{d\theta} \right) \, d\gamma \quad \text{if } \gamma \ll \theta, \gamma \geq 0 \text{ and } \mathbf{H}(\gamma) = \infty \text{ otherwise.}$$

The appropriate choice of  $\theta$  depends on the context at hand; in this article we shall always assume that

$$\theta := \mu \otimes \nu$$

when solving for  $\mathcal{C}^\varepsilon(\mu, \nu)$ . For that problem, the unique minimizer  $\gamma_{\text{opt}}^\varepsilon$  can be written in the form

$$(11) \quad \gamma_{\text{opt}}^\varepsilon = g^\varepsilon \theta, \quad \text{where} \quad g^\varepsilon(x, y) = \exp\left(\frac{-c(x, y) + \alpha(x) + \beta(y)}{\varepsilon}\right),$$

for some Lagrange multipliers  $\alpha, \beta : \mathcal{X} \rightarrow \mathbb{R}$  that realize the marginal constraints (8).  $\alpha$  and  $\beta$  are unique up to a constant additive shift. The marginal constraints imply that  $g^\varepsilon$  is bistochastic in the following sense:

$$(12) \quad \int_{\mathcal{X}} g^\varepsilon(x, y') d\nu(y') = 1, \quad \int_{\mathcal{X}} g^\varepsilon(x', y) d\mu(x') = 1 \quad \text{for } \mu \otimes \nu\text{-almost all } (x, y).$$

This implies the following condition on  $\alpha$ :

$$(13) \quad \alpha(x) = -\varepsilon \cdot \log\left(\int_{\mathcal{X}} \exp\left(\frac{-c(x, y) + \beta(y)}{\varepsilon}\right) d\nu(y)\right)$$

and the equivalent condition for  $\beta$ . These conditions holding  $\mu$ -almost everywhere for  $\alpha$  and  $\nu$ -almost everywhere for  $\beta$  are sufficient and necessary for optimality of  $\gamma^\varepsilon$  as given in (11).

After discretization, these multipliers can be calculated very efficiently via the Sinkhorn algorithm, see below. Another consequence is the loss of sparsity: the support of  $\gamma_{\text{opt}}^\varepsilon$  is that of  $\theta = \mu \otimes \nu$ . When a deterministic transport is sought the diffusivity would be considered a nuisance. But it can also be helpful in reducing discretization artifacts, which is beneficial in our application, and improves the regularity of the map  $\mathcal{C}^\varepsilon$ .

**3.4. Discretization and Sinkhorn algorithm.** When  $\mu$  and  $\nu$  are supported on finite subsets  $\mathcal{M} = \{x_1, \dots, x_M\}$  and  $\mathcal{N} = \{y_1, \dots, y_N\}$  of  $\mathcal{X}$ , then  $\mu$  and  $\nu$  are identified with  $M$ -tuples  $(\mu_1, \dots, \mu_M)$  and  $(\nu_1, \dots, \nu_N)$  of numbers  $\mu_i, \nu_j \geq 0$  that sum up to one. And plans  $\gamma$  can be identified with matrices  $(\gamma_{ij})$  of non-negative entries  $\gamma_{ij} \geq 0$ . The admissibility condition (8) becomes

$$(14) \quad \sum_{j=1}^N \gamma_{ij} = \mu_i \text{ for all } i, \quad \sum_{i=1}^M \gamma_{ij} = \nu_j \text{ for all } j.$$

The reference measure  $\theta$  can also be represented by a discrete matrix of coefficients. With the short-hand notation  $c_{ij} = c(x_i, y_j)$ , the entropic problem (10) becomes

$$(15) \quad \mathcal{C}^\varepsilon(\mu, \nu) = \inf_{\gamma \in \Gamma(\mu, \nu)} \sum_{i,j} \gamma_{ij} (c_{ij} + \varepsilon \log(\gamma_{ij}/\theta_{ij})).$$

with  $\theta_{ij} = \mu_i \nu_j$ . In analogy to (11), its solution is given by

$$(16) \quad \gamma_{ij}^\varepsilon = \exp\left(\frac{-c_{ij} + \alpha_i + \beta_j}{\varepsilon}\right) \cdot \theta_{ij}$$

with Lagrange multipliers  $(\alpha_i)$  and  $(\beta_j)$  to realize the constraint (14). As above,  $(\alpha_i), (\beta_j)$  are unique up to a constant additive shift.

Problem (15) can be solved numerically via the Sinkhorn algorithm [8] which consists of alternately adjusting  $(\alpha_i)$  and  $(\beta_j)$  such that the constraints  $\pi_{\#}^1 \gamma = \mu$  and  $\pi_{\#}^2 \gamma = \nu$  are satisfied, leading to the discretized version of (13). That is, for an initial  $(\beta_j^{(0)})$  (e.g. all zeros) one sets for  $\ell = 1, 2, 3, \dots$ ,

$$(17) \quad \begin{aligned} \exp(\alpha_i^{(\ell)}/\varepsilon) &= \left[ \sum_{j=1}^N \exp\left(\frac{-c_{ij} + \beta_j^{(\ell-1)}}{\varepsilon}\right) \cdot \nu_j \right]^{-1}, \\ \exp(\beta_i^{(\ell)}/\varepsilon) &= \left[ \sum_{i=1}^M \exp\left(\frac{-c_{ij} + \alpha_i^{(\ell)}}{\varepsilon}\right) \cdot \mu_i \right]^{-1}. \end{aligned}$$

#### 4. APPROXIMATION METHOD

We now gradually introduce our method for approximation and spectral analysis of the transfer operator introduced in Section 2. First, we observe that an optimal transport plan also induces a transfer operator (Section 4.1). Then we introduce the entropically smoothed version  $T^\varepsilon : L^p(\mu) \rightarrow L^p(\mu)$  of the original operator  $T$  (Section 4.2) and subsequently its approximate version  $T^{N,\varepsilon} : L^p(\mu^N) \rightarrow L^p(\mu^N)$  (Section 4.3). Finally, we introduce an extension  $\hat{T}^{N,\varepsilon} : L^p(\mu) \rightarrow L^p(\mu)$  of  $T^{N,\varepsilon}$  and show convergence of the extension to  $T^\varepsilon$  in  $L^2$ -operator norm as  $N \rightarrow \infty$  (Section 4.4). This implies convergence of the spectrum of  $\hat{T}^{N,\varepsilon}$  to that of  $T^\varepsilon$  (Section 4.5). The relation between the spectra of  $T^{N,\varepsilon}$  and its extension  $\hat{T}^{N,\varepsilon}$  is elaborated in Section 4.6.

**4.1. Transfer operators induced by transport plans.** A transport plan  $\gamma \in \Gamma(\mu, \nu)$  (computed with or without entropic regularization, or possibly also non-optimal) induces a linear map  $G : L^p(\mu) \rightarrow L^p(\nu)$  characterized by

$$(18) \quad \int_{\mathcal{X}} \varphi(y) (Gh)(y) d\nu(y) = \int_{\mathcal{X} \times \mathcal{X}} \varphi(y) h(x) d\gamma(x, y).$$

With entropic regularization, when  $\gamma = g \cdot (\mu \otimes \nu)$  is of the form (11) one obtains

$$(Gh)(y) = \int_{\mathcal{X}} h(x) g(x, y) d\mu(x).$$

Taking into account (12) and with Jensen's inequality, similar to (5) this yields

$$\int_{\mathcal{X}} J(Gh(y)) d\nu(y) \leq \int_{\mathcal{X} \times \mathcal{X}} J(h(x)) d\gamma(x, y) = \int_{\mathcal{X}} J(h(x)) d\mu(x),$$

and therefore  $G$  indeed maps  $L^p(\mu) \rightarrow L^p(\nu)$ . A similar representation and the same conclusion can be drawn for general  $\gamma \in \Gamma(\mu, \nu)$  by using disintegration [1, Theorem 5.3.1].

**4.2. Entropic regularization of the transfer operator.** For some  $\mu$  let  $T$  be the transfer operator  $L^p(\mu) \rightarrow L^p(F_{\#}\mu)$  as introduced in Section 2.4. We do not necessarily assume  $F_{\#}\mu = \mu$ . Let  $\gamma^\varepsilon$  be the optimal  $\varepsilon$ -entropic transport plan between  $F_{\#}\mu$  and  $\mu$ , i.e. the minimizer corresponding to (10), and let  $g^\varepsilon$  be its density, i.e.  $\gamma^\varepsilon = g^\varepsilon \cdot (F_{\#}\mu) \otimes \mu$ , see (11). In this case the marginal conditions (12) become

$$(19) \quad \int_{\mathcal{X}} g^\varepsilon(x', x) dF_{\#}\mu(x') = 1, \quad \int_{\mathcal{X}} g^\varepsilon(y, y') d\mu(y') = 1.$$

for  $\mu$ -almost all  $x$  and  $F_{\#}\mu$ -almost all  $y$ .

As discussed in Section 4.1,  $\gamma^\varepsilon$  induces a map  $L^p(F_{\#}\mu) \rightarrow L^p(\mu)$  which we will denote by  $G^\varepsilon$ . It is given by

$$(20) \quad (G^\varepsilon h)(y) = \int_{\mathcal{X}} h(x) g^\varepsilon(x, y) dF_{\#}\mu(x).$$

Now, set  $T^\varepsilon := G^\varepsilon T$  as the concatenation of the two maps, which takes  $L^p(\mu)$  into itself. This is illustrated in Figure 2, left. Using (4) we obtain the representation

$$(21) \quad \begin{aligned} (T^\varepsilon h)(y) &= (G^\varepsilon Th)(y) = \int_{\mathcal{X}} (Th)(x) g^\varepsilon(x, y) dF_{\#}\mu(x) \\ &= \int_{\mathcal{X}} g^\varepsilon(x, y) dF_{\#}(h\mu)(x) = \int_{\mathcal{X}} g^\varepsilon(F(x), y) h(x) d\mu(x). \end{aligned}$$

Using (19) one finds that the measure  $g^\varepsilon(F(\cdot), \cdot) \cdot \mu \otimes \mu$  lies in  $\Gamma(\mu, \mu)$  and by the form of the density  $g^\varepsilon(F(\cdot), \cdot)$ ,

$$(22) \quad g^\varepsilon(F(x), y) = \exp\left(\frac{-c(F(x), y) + \alpha(F(x)) + \beta(y)}{\varepsilon}\right),$$

we deduce that it is the optimal  $\varepsilon$ -entropic coupling between  $\mu$  and itself with respect to the cost function  $c(F(\cdot), \cdot)$  and  $\theta = \mu \otimes \mu$ , see (11). We will denote the density as

$$(23) \quad t^\varepsilon(x, y) := g^\varepsilon(F(x), y).$$

We clarify the consistency of the definition  $T^\varepsilon : L^p(\mu) \rightarrow L^p(\mu)$  in (21) with the classical transfer operator  $T : L^p(\mu) \rightarrow L^p(F_{\#}\mu)$  from (3) in the limit  $\varepsilon \downarrow 0$ . We assume for simplicity that the unregularized optimal transport  $\gamma^0$  from  $F_{\#}\mu$  to  $\mu$  is given by an invertible transport map  $\Psi : \mathcal{X} \rightarrow \mathcal{X}$ , i.e.  $\gamma^0 = (\text{id}, \Psi)_{\#} F_{\#}\mu$ . In that case, as  $\varepsilon \downarrow 0$ , the entropic optimal plan  $\gamma^\varepsilon$  converges weakly to  $\gamma^0$ , see for instance [6]. Now let  $\varphi \in C(\mathcal{X})$  be a test function, and assume that  $h \in L^p(F_{\#}\mu)$  is continuous. The definitions of  $T^\varepsilon$  from (21) and

of  $T$  from (4) imply:

$$\begin{aligned}
\int_{\mathcal{X}} \varphi(y) (T^\varepsilon h)(y) d\mu(y) &= \int_{\mathcal{X} \times \mathcal{X}} \varphi(y) (Th)(x) g^\varepsilon(x, y) d(F_{\#}\mu \otimes \mu)(x, y) \\
&= \int_{\mathcal{X} \times \mathcal{X}} \varphi(y) (Th)(x) d\gamma^\varepsilon(x, y) \\
&\xrightarrow{\varepsilon \rightarrow 0} \int_{\mathcal{X} \times \mathcal{X}} \varphi(y) (Th)(x) d\gamma^0(x, y) \\
&= \int_{\mathcal{X}} \varphi \circ \Psi(x) (Th)(x) dF_{\#}\mu(x),
\end{aligned}$$

which in view of  $\Psi_{\#}F_{\#}\mu = \mu$  implies that  $\mu$ -a.e. the limit of  $T^\varepsilon h$  is  $(Th) \circ \Psi^{-1}$ . That is, the limit of the modified transfer operators  $T^\varepsilon$  coincides (at least formally) with the unregularized transfer operator  $T$ , concatenated with the optimal transport map from  $\mu$  to  $F_{\#}\mu$ . In particular, if  $\mu$  is invariant under  $F$ , then the optimal map  $\Psi$  is the identity, and  $T^\varepsilon$  converges to  $T$ . In that case, for small positive  $\varepsilon > 0$ , the operator  $T^\varepsilon$  should be thought of as a regularized version of  $T$ , where  $(T^\varepsilon h)(x)$  is a weighted average of the values  $h(y)$  for  $y$  close to  $F^{-1}(x)$ .

**4.3. Approximate entropic transfer operator.** Let now  $(\mu^N)_N$  be an approximating sequence of  $\mu$ , i.e.  $\mu^N \xrightarrow{*} \mu$  as  $N \rightarrow \infty$ . In our applications we consider  $\mu^N$  that are concentrated on a finite number  $N$  of points  $x_1^N, \dots, x_N^N \in \mathcal{X}$ ,

$$(24) \quad \mu^N := \sum_{k=1}^N m_k^N \delta_{x_k^N} \quad \text{with} \quad m_k^N \geq 0 \quad \text{and} \quad \sum_{k=1}^N m_k^N = 1.$$

$F_{\#}\mu$  is then given by  $\sum_{k=1}^N m_k^N \delta_{F(x_k^N)}$ . But the analysis in this section works for general  $\mu^N \in \mathcal{P}(\mathcal{X})$ . The measure  $\mu^N$  induces the discrete transfer operator  $T^N : L^p(\mu^N) \rightarrow L^p(F_{\#}\mu^N)$  via (3). We can then perform the same construction as in the previous section for the measure  $\mu^N$ , introducing an operator  $G^{N,\varepsilon} : L^p(F_{\#}\mu^N) \rightarrow L^p(\mu^N)$  (via the entropic optimal transport plan  $\gamma^{N,\varepsilon}$  from  $F_{\#}\mu^N$  to  $\mu^N$ ) and concatenating it with  $T^N$  to obtain the operator  $T^{N,\varepsilon}$  from  $L^p(\mu^N)$  onto itself. This is part of the illustration in Figure 2, right. Analogously to (21), (23) we find that

$$(T^{N,\varepsilon} h)(y) = \int_{\mathcal{X}} h(x) t^{N,\varepsilon}(x, y) d\mu^N(x)$$

$\mu^N$ -almost everywhere, where  $t^{N,\varepsilon}$  is the density of the optimal  $\varepsilon$ -entropic transport plan between  $\mu^N$  and itself for the cost  $c(F(\cdot), \cdot)$ . For the discrete case (24) this becomes

$$(25) \quad (T^{N,\varepsilon} h)(x_k^N) = \sum_{j=1}^N h(x_j^N) t^{N,\varepsilon}(x_j^N, x_k^N) m_j^N$$

In this case  $t^{N,\varepsilon}$  can be identified with a bistochastic  $N \times N$  matrix  $(t^{N,\varepsilon}(x_k^N, x_j^N))_{j,k=1}^N$  where bistochastic has to be understood relative to the weights  $(m_k^N)$ , i.e.,

$$\sum_{j=1}^N m_j^N t^{N,\varepsilon}(x_k^N, x_j^N) = 1, \quad \sum_{k=1}^N m_k^N t^{N,\varepsilon}(x_k^N, x_j^N) = 1.$$

This matrix can be approximated numerically efficiently by the Sinkhorn algorithm, see Section 3.4.

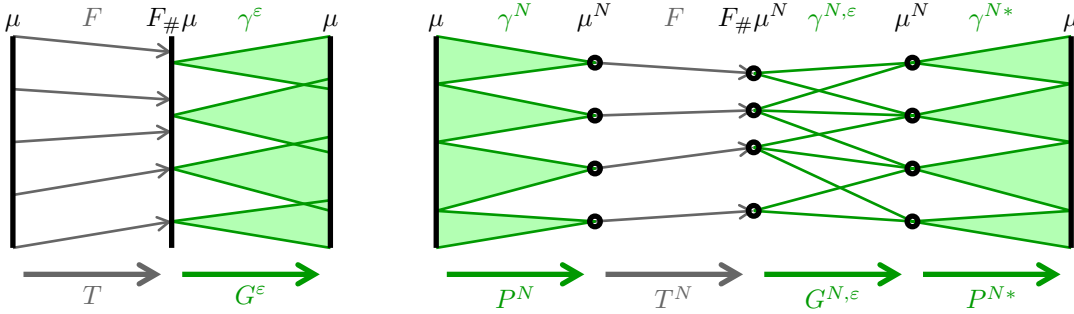


FIGURE 2. Schematic of the construction of the maps  $T^\varepsilon$  (left) and  $\hat{T}^{N,\varepsilon}$  (right). In this figure  $\gamma^\varepsilon$  is a non-deterministic (entropic) continuous to continuous transport plan,  $\gamma^N$  is a deterministic unregularized continuous to discrete transport plan and  $\gamma^{N,\varepsilon}$  is a non-deterministic discrete to discrete transport plan.

**4.4. Convergence as  $N \rightarrow \infty$ .** For better comparison of the transfer operators  $T^\varepsilon$  and  $T^{N,\varepsilon}$  related to a measure  $\mu$  and its approximation  $\mu^N$ , we will now extend the latter to the space  $L^p(\mu)$ . Let now  $\gamma^N$  be the optimal (non-entropic) transport plan between  $\mu$  and  $\mu^N$ . As discussed in Section 4.1 it induces an operator  $L^p(\mu) \rightarrow L^p(\mu^N)$  which we will denote by  $P^N$ . We now set

$$\hat{T}^{N,\varepsilon} := P^{N*} T^{N,\varepsilon} P^N$$

where  $P^{N*} : L^p(\mu^N) \rightarrow L^p(\mu)$  is the adjoint of  $P^N$  in the case  $p = 2$ . It is equal to the transfer operator induced by the ‘transpose’  $(\pi_2, \pi_1)\#\gamma^N$  of the transport plan  $\gamma^N$ . The structure of the operator  $\hat{T}^{N,\varepsilon}$  is illustrated in Figure 2, right. One finds

$$\int_{\mathcal{X}} (\hat{T}^{N,\varepsilon} h)(y) \varphi(y) d\mu(y) = \int_{\mathcal{X}^4} h(x) t^{N,\varepsilon}(v, w) \varphi(y) d\gamma^N(x, v) d\gamma^N(y, w)$$

for test functions  $\varphi \in C(\mathcal{X})$ . Equivalently we can write

$$(26) \quad \begin{aligned} (\hat{T}^{N,\varepsilon}h)(y) &= \int_{\mathcal{X}} h(x) \hat{t}^{N,\varepsilon}(x, y) \, d\mu(x) \\ \text{with } \hat{t}^{N,\varepsilon}(x, y) &:= \int_{\mathcal{X} \times \mathcal{X}} t^{N,\varepsilon}(v, w) \, d\gamma_x^N(v) \, d\gamma_y^N(w) \end{aligned}$$

where  $(\gamma_x^N)_x$  is the disintegration of  $\gamma^N$  with respect to its first marginal, i.e.

$$\int_{\mathcal{X} \times \mathcal{X}} \varphi(x, y) \, d\gamma^N(x, y) = \int_{\mathcal{X}} \left[ \int_{\mathcal{X}} \varphi(x, y) \, d\gamma_x^N(y) \right] \, d\mu(x)$$

for  $\varphi \in C(X \times Y)$ . Note that since all  $(\gamma_x^N)_x$  are probability measures and since  $t^{N,\varepsilon} \in L^\infty(\mu^N \otimes \mu^N)$ , one finds that  $\hat{t}^{N,\varepsilon} \in L^p(\mu \otimes \mu)$  for any  $p \in [1, \infty]$ .

**Proposition 1.** *If  $\mu^N \xrightarrow{*} \mu$  as  $N \rightarrow \infty$  then  $\|\hat{t}^{N,\varepsilon} - t^\varepsilon\|_{L^2(\mu \otimes \mu)} \rightarrow 0$  and  $\hat{T}^{N,\varepsilon} \rightarrow T^\varepsilon$  in the  $L^2(\mu) \rightarrow L^2(\mu)$  operator norm.*

*Proof.* In order to estimate the difference of  $\hat{T}^{N,\varepsilon}$  and  $T^\varepsilon$  in the operator norm, let  $h \in L^2(\mu)$  be given and estimate as follows:

$$\begin{aligned} \|\hat{T}^{N,\varepsilon}h - T^\varepsilon h\|_{L^2(\mu)}^2 &= \int_{\mathcal{X}} \left| \int_{\mathcal{X}} (\hat{t}^{N,\varepsilon}(y, x) - t^\varepsilon(y, x)) h(y) \, d\mu(y) \right|^2 \, d\mu(x) \\ &\leq \int_{\mathcal{X}} \left[ \int_{\mathcal{X}} (\hat{t}^{N,\varepsilon}(y, x) - t^\varepsilon(y, x))^2 \, d\mu(y) \int_{\mathcal{X}} h(y)^2 \, d\mu(y) \right] \, d\mu(x) \\ &= \|\hat{t}^{N,\varepsilon} - t^\varepsilon\|_{L^2(\mu \otimes \mu)}^2 \|h\|_{L^2(\mu)}^2. \end{aligned}$$

That is, we have

$$\|T^{N,\varepsilon} - T^\varepsilon\|_{L^2(\mu) \rightarrow L^2(\mu)} \leq \|\hat{t}^{N,\varepsilon} - t^\varepsilon\|_{L^2(\mu \otimes \mu)}.$$

Therefore we now proceed to prove that the latter tends to zero. For each  $N$ , let  $\alpha^N$  and  $\beta^N$  be the optimal scaling factors for the  $\varepsilon$ -entropic optimal transport between  $\mu^N$  and itself for cost function  $\hat{c} := c(F(\cdot), \cdot)$  and  $\theta = \mu^N \otimes \mu^N$ , as specified in (16). By the optimality condition for  $\alpha^N$  (14) one has  $\mu^N(x)$ -almost everywhere

$$(27) \quad \alpha^N(x) = -\varepsilon \cdot \log \left( \int_{\mathcal{X}} \exp \left( \frac{-\hat{c}(x, y) + \beta^N(y)}{\varepsilon} \right) \, d\mu^N(y) \right).$$

Note that the right-hand side can be evaluated for any  $x \in \mathcal{X}$ , not just  $\mu^N$ -almost everywhere, and thus we can extend  $\alpha^N$  to a function  $\mathcal{X} \rightarrow \mathbb{R}$ .

By compactness of  $\mathcal{X}$  and continuity of  $F$ ,  $\hat{c}$  is uniformly continuous on  $\mathcal{X} \times \mathcal{X}$ . This means there exists a modulus of continuity  $\omega$  ( $\omega$  is a continuous, concave map  $\mathbb{R}_+ \rightarrow \mathbb{R}_+$  with  $\omega(0) = 0$ ), such that

$$|\hat{c}(x, y) - \hat{c}(x', y')| \leq \omega(\sqrt{d(x, x')^2 + d(y, y')^2}).$$

One quickly verifies that  $\alpha^N$  inherits the modulus of continuity from  $\hat{c}$  by estimates of the form

$$\begin{aligned} \alpha^N(x') &\leq -\varepsilon \cdot \log \left( \int_{\mathcal{X}} \exp \left( \frac{-\hat{c}(x, y) - \omega(d(x, x')) + \beta^N(y)}{\varepsilon} \right) d\mu^N(y) \right) \\ &= \alpha^N(x) + \omega(d(x, x')). \end{aligned}$$

For instance, when  $\hat{c}$  is Lipschitz continuous, then so will be  $\alpha^N$ . In the same way we extend the scaling factor  $\beta^N$  to  $\mathcal{X}$ , also inheriting the modulus of continuity from  $\hat{c}$ . Note that this argument can also be extended to the case  $\varepsilon = 0$ .

Therefore, by fixing the additive shift invariance, e.g. by fixing  $\alpha^N(x_0) = 0$  for some fixed  $x_0 \in \mathcal{X}$ , the pair of sequences of functions  $(\alpha^N)$  and  $(\beta^N)$  is uniformly bounded and uniformly equicontinuous and thus by the Arzelà–Ascoli theorem there exists a convergent subsequence with limits  $\alpha$  and  $\beta$  for the uniform convergence. By going to the limit (weak\* convergence of  $\mu^N$  and uniform convergence of  $\alpha^N$  and  $\beta^N$ ) in (27) and its counterpart for the second marginal we find that  $\alpha$  and  $\beta$  are optimal scaling factors for the limit problem between  $\mu$  and itself. Therefore,  $\alpha$  and  $\beta$  are unique, up to constant shifts, which we have eliminated by the condition  $\alpha(x_0) = \lim_{N \rightarrow \infty} \alpha^N(x_0)$ . Consequently, the whole sequence converges to  $\alpha$  and  $\beta$ . The extension of  $(\alpha^N, \beta^N)$  carries over to  $t^{N, \varepsilon}(x, y) = \exp \left( \frac{-\hat{c}(x, y) + \alpha^N(x) + \beta^N(y)}{\varepsilon} \right)$ . And consequently  $t^{N, \varepsilon}$  converges uniformly to  $t^\varepsilon$  and all  $t^{N, \varepsilon}$  have a common modulus of continuity (obtained by combining the moduli of  $\alpha^N$ ,  $\beta^N$  and  $\hat{c}$ , and the exponential map  $\exp(\cdot/\varepsilon)$ ) which for simplicity we will denote again by  $\omega$ , i.e. there exists a continuous, concave  $\omega : \mathbb{R}_+ \rightarrow \mathbb{R}_+$  with  $\omega(0) = 0$  such that

$$(28) \quad |t^{N, \varepsilon}(x, y) - t^{N, \varepsilon}(x', y')| \leq \omega(\sqrt{d(x, x')^2 + d(y, y')^2}).$$

Since  $\mathcal{X}$  is compact,  $\omega$  can be assumed to be bounded, and thus equivalently we may demand that

$$(29) \quad |t^{N, \varepsilon}(x, y) - t^{N, \varepsilon}(x', y')|^2 \leq \hat{\omega}(d(x, x')^2 + d(y, y')^2).$$

where  $\hat{\omega}$  is the concave hull of  $[\omega(\sqrt{\cdot})]^2$  and still continuous at  $\hat{\omega}(0) = 0$ . This form will be more convenient in the following. Note that the densities  $t^{N, \varepsilon}$  and  $t^\varepsilon$  only exist for  $\varepsilon > 0$ , and their modulus of continuity deteriorates as  $\varepsilon \rightarrow 0$ .

We can now estimate

$$\|\hat{t}^{N, \varepsilon} - t^\varepsilon\|_{L^2(\mu \otimes \mu)} \leq \|\hat{t}^{N, \varepsilon} - t^{N, \varepsilon}\|_{L^2(\mu \otimes \mu)} + \|t^{N, \varepsilon} - t^\varepsilon\|_{L^2(\mu \otimes \mu)}.$$

The second term tends to zero as  $N \rightarrow \infty$  by the uniform convergence of  $t^{N, \varepsilon} \rightarrow t^\varepsilon$  on  $\mathcal{X} \times \mathcal{X}$ . For the first term we estimate, by using the representation (26), the bound (29), Jensen's inequality for convex and concave functions, and the fact that  $\gamma^N$  is an optimal

transport plan for the 2-Wasserstein distance between  $\mu$  and  $\mu^N$ ,

$$\begin{aligned} \|\hat{t}^{N,\varepsilon} - t^{N,\varepsilon}\|_{L^2}^2 &= \int_{\mathcal{X} \times \mathcal{X}} \left| \int_{\mathcal{X} \times \mathcal{X}} [t^{N,\varepsilon}(v, w) - t^{N,\varepsilon}(x, y)] d\gamma_x^N(v) d\gamma_y^N(w) \right|^2 d\mu(x) d\mu(y) \\ &\leq \int_{\mathcal{X}^4} |t^{N,\varepsilon}(v, w) - t^{N,\varepsilon}(x, y)|^2 d\gamma^N(x, v) d\gamma^N(y, w) \\ &\leq \int_{\mathcal{X}^4} \hat{\omega} (d(x, v)^2 + d(y, w)^2) d\gamma^N(x, y) d\gamma^N(y, w) \\ &\leq \hat{\omega} (2W_2^2(\mu, \mu^N)). \end{aligned}$$

This tends to zero by the assumption  $\mu^N \xrightarrow{*} \mu$ , see Section 3.2.  $\square$

#### 4.5. Compactness and convergence of spectrum.

**Proposition 2.** *The operator  $T^\varepsilon : L^2(\mu) \rightarrow L^2(\mu)$  is compact.*

*Proof.* As shown in Section 4.2,  $T^\varepsilon$  is given by

$$(T^\varepsilon h)(y) = \int_{\mathcal{X}} h(x) g^\varepsilon(F(x), y) d\mu(x).$$

Due to the marginal constraints (19) we have

$$\int_{\mathcal{X}} \int_{\mathcal{X}} g^\varepsilon(F(x), y)^2 d\mu(x) d\mu(y) = 1,$$

so that  $T^\varepsilon$  is a Hilbert-Schmidt operator and as such compact.  $\square$

Compactness of  $T^\varepsilon$  together with convergence of  $\hat{T}^{N,\varepsilon}$  to  $T^\varepsilon$  in the  $L^2$ -operator norm yields that the eigenpairs of  $\hat{T}^{N,\varepsilon}$  converge to those of  $T^\varepsilon$  as  $N \rightarrow \infty$ : Let  $\lambda_1^\varepsilon, \lambda_2^\varepsilon, \dots$  be the nonzero eigenvalues of  $T^\varepsilon$  (taking into account their algebraic multiplicities). One can order the eigenvalues  $\hat{\lambda}_1^{N,\varepsilon}, \hat{\lambda}_2^{N,\varepsilon}, \dots$  (depending on  $N$ ) of  $\hat{T}^{N,\varepsilon}$  such that for each  $k$ ,  $\hat{\lambda}_k^{N,\varepsilon} \rightarrow \lambda_k^\varepsilon$  as  $N \rightarrow \infty$  [11]. For the eigenfunctions, Corollary 1 in [3] directly gives the following result:

**Theorem 2.** *Let  $\hat{\lambda}^{N,\varepsilon}$  be an eigenvalue of  $\hat{T}^{N,\varepsilon}$  such that  $\hat{\lambda}^{N,\varepsilon} \rightarrow \lambda^\varepsilon$  as  $N \rightarrow \infty$  with associated normalized eigenfunction  $\hat{\varphi}^{N,\varepsilon}$ . Then, for  $N$  large enough, there is an eigenfunction  $\varphi^\varepsilon$  of  $T^\varepsilon$  at the eigenvalue  $\lambda^\varepsilon$  and a constant  $C > 0$  independent of  $N$  such that*

$$\|\hat{\varphi}^{N,\varepsilon} - \varphi^\varepsilon\|_{L^2} \leq C \|\hat{T}^{N,\varepsilon} - T^\varepsilon\|_{L^2}.$$

Note that the construction of  $T^{N,\varepsilon}$  and  $\hat{T}^{N,\varepsilon}$  can also be performed in the limit case  $\varepsilon = 0$ , but in that case one does in general not observe convergence towards  $T^{\varepsilon=0} = T$  as  $N \rightarrow \infty$  (and  $T$  is usually not compact).

**4.6. Relation between the spectra of  $T^{N,\varepsilon}$  and  $\hat{T}^{N,\varepsilon}$ .** Recall the optimal transport plan  $\gamma^N$  between  $\mu$  and  $\mu^N$  and the induced operator  $P^N : L^p(\mu) \rightarrow L^p(\mu^N)$  as introduced in Section 4.4 and consider the case where  $\gamma_x^N = \delta_{\Phi(x)}$  for  $\mu$ -a.e.  $x$ , that is, for almost all  $x$ , all the mass of  $\mu$  at  $x$  is transported to  $\Phi(x)$  for some measurable  $\Phi : \mathcal{X} \rightarrow \mathcal{X}$ . This map  $\Phi$  then solves the Monge problem (7) and it exists, for instance, when  $\mathcal{X} \subset \mathbb{R}^d$  and  $\mu$  is dominated by the Lebesgue measure, see [20] for an adaptation to Riemannian manifolds. In this case  $(P^{N*}h)(x) = h(\Phi(x))$   $\mu$ -a.e., i.e. the function  $P^{N*}h$  is piecewise constant on preimages of points under  $\Phi$  (these preimages may be individual points, in which case piecewise constancy is irrelevant). Conversely, for a function  $h \in L^2(\mu)$  that is piecewise constant on preimages of single points under  $\Phi$ , we find  $(P^N h)(x) = h(\Phi^{-1}(x))$ .  $P^N$  is zero on the orthogonal complement of that space. Therefore, for each eigenpair  $(h, \lambda) \in L^2(\mu^N) \otimes \mathbb{C}$  of  $T^{N,\varepsilon}$ ,  $(h \circ \Phi, \lambda)$  is an eigenpair of  $\hat{T}^{N,\varepsilon}$  and all other eigenvalues of  $\hat{T}^{N,\varepsilon}$  are zero. In this case, when  $\mu^N$  is supported on a finite number of points, the spectrum of  $\hat{T}^{N,\varepsilon}$  (which converges to that of  $T^\varepsilon$ ), can be studied via the discrete matrix representation of  $T^{N,\varepsilon}$ .

It might happen however that  $\gamma^N$  is not induced by a map  $\Phi$  in which case the direct correspondence between the spectra of  $T^{N,\varepsilon}$  and  $\hat{T}^{N,\varepsilon}$  fails. When  $\mathcal{X} \subset \mathbb{R}^d$  and  $\mu$  is atomless this can be remedied as follows: By [25, Theorem 1.32] for each  $N$  there exists a transport plan  $\tilde{\gamma}^N$  that is induced by a map  $\tilde{\Phi}^N$  such that  $\int_{\mathcal{X}^2} c(x, y) d\tilde{\gamma}^N(x, y) = \int_{\mathcal{X}} c(x, \tilde{\Phi}^N(x)) d\mu(x) \rightarrow 0$  as  $N \rightarrow \infty$ . Let  $\tilde{P}^N$  be the corresponding transfer operator, which can be used to define an alternative extension  $\tilde{T}^{N,\varepsilon}$  of  $T^{N,\varepsilon}$ . As argued above, these two operators will have the same non-zero eigenvalues and the corresponding eigenvectors are connected via  $\tilde{\Phi}^N$ . By the same arguments as in Proposition 1 one will find  $\tilde{T}^{N,\varepsilon} \rightarrow T^\varepsilon$  in operator norm. Hence, the spectrum of  $T^{N,\varepsilon}$  still converges to that of  $T^\varepsilon$ .

## 5. PROOF OF CONCEPT — ANALYSIS OF THE SHIFT MAP ON THE TORUS

Below, we use the following short-hand notation for vectors  $v = (v_1, \dots, v_d) \in \mathbb{C}^d$ :

$$[v]^2 = v^T v = \sum_{\alpha=1}^d v_\alpha^2.$$

If  $v \in \mathbb{R}^d \subset \mathbb{C}^d$ , then  $[v]^2 = |v|^2$ , but in general,  $[v]^2$  is a complex number.

**5.1. The shift map on the  $d$ -torus.** On the  $d$ -dimensional torus  $\mathcal{X} = \mathbb{R}^d / \mathbb{Z}^d$ , we consider the shift map  $F(x) = x + \theta$  with a fixed vector  $\theta \in (-1/2, +1/2)^d$ . The uniform measure  $\mu$  on  $\mathcal{X}$  is clearly invariant under  $F$ .

**Remark 1.** *If  $\theta$  happens to be irrational, then  $\mu$  is the unique invariant  $F$ -measure, and  $F$  is quasi-periodic on  $\mathcal{X}$ . For the discussion below, these properties are not important.*

The transfer operator is given by

$$(Tf)(x) = f(x - \theta).$$

A complete basis of eigenfunctions is formed by  $\varphi_k(x) = e^{2\pi i k \cdot x}$  for  $k \in \mathbb{Z}^d$ , with respective eigenvalues

$$(30) \quad \lambda_k = e^{-2\pi i k \cdot \theta}.$$

Indeed,

$$(T\varphi_k)(x) = \varphi_k(x - \theta) = e^{2\pi i k \cdot (x - \theta)} = e^{-2\pi i k \cdot \theta} \varphi_k(x).$$

For the distance of points  $x, x' \in \mathcal{X}$ , we use

$$d(x, x') := \min_{k \in \mathbb{Z}^d} |\hat{x}' - \hat{x} + k|,$$

where  $\hat{x}, \hat{x}' \in \mathbb{R}^d$  are any representatives of  $x, x'$ , and  $|\cdot|$  is the Euclidean distance on  $\mathbb{R}^d$ . Equivalently: define the fundamental domain

$$\mathbf{C} := (-1/2, +1/2]^d.$$

Choose representatives  $\hat{x}, \hat{x}' \in \mathbb{R}^d$  of  $x, x' \in \mathcal{X}$  such that  $\hat{x}' \in \hat{x} + \mathbf{C}$ . Then  $d(x, x') = |\hat{x} - \hat{x}'|$ .

**5.2. Spectrum of the regularized transfer operator.** Thanks to the extremely high symmetry of the problem, the kernel  $t^\varepsilon$  can be calculated almost explicitly: it follows that the scaling factors  $\alpha$  and  $\beta$  are constant in space<sup>3</sup>, and thus by (22) and (23):

$$(31) \quad t^\varepsilon(x, y) = g^\varepsilon(F(x), y) = \frac{1}{Z_\varepsilon} e^{-d^2(x+\theta, y)/\varepsilon}, \quad Z_\varepsilon := \varepsilon^{d/2} \int_{\varepsilon^{-1/2}\mathbf{C}} e^{-|\zeta|^2} d\zeta.$$

Provided  $y \in x + \theta + \mathbf{C}$ , this can be written more explicitly:

$$t^\varepsilon(x, y) = \frac{1}{Z_\varepsilon} e^{-|x+\theta-y|^2/\varepsilon}$$

**Proposition 3.** *For any  $\varepsilon > 0$ , a complete system of eigenfunctions of  $T^\varepsilon$  is given by the  $\varphi_k$ . The respective eigenvalues  $\lambda_k^\varepsilon$  satisfy*

$$(32) \quad |\lambda_k^\varepsilon - e^{-\pi^2 \varepsilon |k|^2} \lambda_k| \leq 2^{d+1} e^{-\frac{1}{8\varepsilon}},$$

*uniformly for  $0 < \varepsilon < 1/(8(d+2)\ln 2)$ . Above, the  $\lambda_k$  are given by (30).*

This result shows the interplay of two length scales. Based on (31) we see that  $T^\varepsilon$  acts locally like a translation by  $\theta$  (given by  $F$  or  $T$ ) and a subsequent convolution with a Gaussian kernel of width  $\sqrt{\varepsilon}$ , which is the length scale of the blur introduced by entropic optimal transport. On the other side,  $1/|k|$  is the periodicity length scale of the eigenfunction  $\varphi_k$ . Proposition 3 states that for small  $\varepsilon > 0$ , the corresponding eigenvalues of  $T^\varepsilon$  and of  $T$  are similar for eigenfunctions with length scale above the blur scale, i.e.  $\sqrt{\varepsilon} \ll 1/|k|$ .

---

<sup>3</sup>Because  $\alpha$  and  $\beta$  are (up to constant shifts) the unique maximizers of a dual problem of (10) and must therefore be constant by symmetry of the problem.

*Proof.* Clearly, each  $\varphi_k$  is an eigenfunction since

$$\begin{aligned}
(T^\varepsilon \varphi_k)(y) &= \int_{\mathcal{X}} e^{2\pi i k \cdot x} t^\varepsilon(x, y) dx \\
&= \frac{1}{Z_\varepsilon} \int_{y-\theta+\mathbf{C}} e^{-|x-y+\theta|^2/\varepsilon+2\pi i k \cdot x} dx \\
&= \left( \frac{1}{Z_\varepsilon} \int_{y-\theta+\mathbf{C}} \exp\left(-\frac{1}{\varepsilon}|x-y+\theta|^2 + 2\pi i k \cdot (x-y+\theta)\right) dx \right) e^{2\pi i k \cdot (y-\theta)} \\
&= \left( \frac{1}{Z_\varepsilon} \int_{\mathbf{C}} \exp\left(-\left[\frac{z}{\sqrt{\varepsilon}} - \sqrt{\varepsilon}\pi i k\right]^2\right) e^{-\varepsilon\pi^2|k|^2} dz \right) \lambda_k \varphi_k(y) \\
&= \left( \frac{\sqrt{\varepsilon}^d}{Z_\varepsilon} \int_{\varepsilon^{-1/2}\mathbf{C}} e^{-[\zeta-i\sqrt{\varepsilon}\pi k]^2} d\zeta \right) e^{-\varepsilon\pi^2|k|^2} \lambda_k \varphi_k(y).
\end{aligned}$$

To prove the claimed asymptotics, we start by observing that for each  $\zeta, \tau \in \mathbb{R}^d$  with  $\zeta \in \mathbb{R}^d \setminus \varepsilon^{-1/2}\mathbf{C}$ :

$$(33) \quad |e^{-[\zeta-i\tau]^2}| = e^{|\tau|^2-|\zeta|^2} \leq e^{|\tau|^2} e^{-\frac{1}{8\varepsilon}} e^{-\frac{1}{2}|\zeta|^2},$$

since  $|\zeta|^2 \geq \frac{1}{4\varepsilon}$ . Using that, independently of  $\tau$ ,

$$(34) \quad \int_{\mathbb{R}^d} e^{-[\zeta-i\tau]^2} d\zeta = \pi^{d/2},$$

we thus obtain the following bound:

$$\begin{aligned}
(35) \quad \left| \pi^{d/2} - \int_{\varepsilon^{-1/2}\mathbf{C}} e^{-[\zeta-i\tau]^2} d\zeta \right| &= \left| \int_{\mathbb{R}^d \setminus \varepsilon^{-1/2}\mathbf{C}} e^{-[\zeta-i\tau]^2} d\zeta \right| \\
&\leq e^{|\tau|^2} e^{-\frac{1}{8\varepsilon}} \int_{\mathbb{R}^d} e^{-\frac{1}{2}|\zeta|^2} d\zeta = (2\pi)^{d/2} e^{|\tau|^2} e^{-\frac{1}{8\varepsilon}}.
\end{aligned}$$

Apply this with  $\tau = 0$  to obtain

$$Z_\varepsilon \geq (\pi\varepsilon)^{d/2} - (2\pi\varepsilon)^{d/2} e^{-\frac{1}{8\varepsilon}} = (\pi\varepsilon)^{d/2} (1 - 2^{d/2} e^{-\frac{1}{8\varepsilon}}),$$

and in particular we have  $Z_\varepsilon \geq (\pi\varepsilon/2)^{d/2} > 0$  for all  $\varepsilon > 0$  in the range specified in the claim. Apply (35) again, now with  $\tau = \sqrt{\varepsilon}\pi k$ , to obtain

$$\left| (\pi\varepsilon)^{d/2} - \varepsilon^{d/2} \int_{\varepsilon^{-1/2}\mathbf{C}} e^{-[\zeta-i\sqrt{\varepsilon}\pi k]^2} d\zeta \right| \leq (2\pi\varepsilon)^{d/2} e^{\varepsilon\pi^2|k|^2} e^{-\frac{1}{8\varepsilon}}.$$

Divide this inequality by  $Z_\varepsilon$ . Using that  $Z_\varepsilon^{-1} \leq (\pi\varepsilon/2)^{-d/2}$  on the one hand, that, by (35) for  $\tau = 0$ ,

$$\left| 1 - \frac{(\pi\varepsilon)^{d/2}}{Z_\varepsilon} \right| \leq \frac{(2\pi\varepsilon)^{d/2} e^{-1/(8\varepsilon)}}{Z_\varepsilon} \leq 2^d e^{-\frac{1}{8\varepsilon}},$$

on the other hand, and finally that  $e^{\pi^2 \varepsilon |k|} \geq 1$ , we conclude that

$$\left| 1 - \frac{\varepsilon^{d/2}}{Z_\varepsilon} \int_{\varepsilon^{-1/2} \mathbf{C}} e^{-[\zeta - i\sqrt{\varepsilon} \pi k]^2} d\zeta \right| \leq 2^{d+1} e^{\varepsilon \pi^2 |k|^2} e^{-\frac{1}{8\varepsilon}}.$$

Since  $|\lambda_k| = 1$ , this yields the claim (32).  $\square$

**5.3. Spectrum of the discretized regularized transfer operator.** For the discretization, we consider a regular lattice with  $N = n^d$  points  $x_j^N$  in the fundamental domain  $\mathbf{C}$ . Specifically, let  $J_N \subset \mathbb{Z}^d$  be the set of indices  $j = (j_1, \dots, j_d)$  such that

$$x_j^N = (j_1/n, \dots, j_d/n) \in \mathbf{C}.$$

All points  $x_j^N$  are given equal weight  $m_j^N = 1/N$ , thus

$$\mu^N = \frac{1}{N} \sum_{j \in \mathbb{Z}_n^d} \delta_{x_j^N}.$$

Based on (25) we introduce the matrix  $\Gamma^{N,\varepsilon}$  via

$$\Gamma_{\ell,m}^{N,\varepsilon} := t^{N,\varepsilon}(x_m^N, x_\ell^N) m_m^N.$$

Spectral analysis of  $T^{N,\varepsilon}$  then is equivalent to spectral analysis of  $\Gamma^{N,\varepsilon}$ . As before, the high symmetry of the problem implies that the weight factors  $\alpha$  and  $\beta$  in the representation (22) are actually global constants, and thus

$$\Gamma_{\ell,m}^{N,\varepsilon} = \frac{1}{N Z^{N,\varepsilon}} \exp\left(-\frac{1}{\varepsilon} d(x_m^N + \theta, x_\ell^N)^2\right),$$

with a normalization constant

$$(36) \quad Z^{N,\varepsilon} = \frac{1}{N} \sum_{m \in J_N} \exp\left(-\frac{1}{\varepsilon} d(x_m^N + \theta, 0)^2\right).$$

**Proposition 4.** *A complete system of eigenvectors for  $\Gamma^{N,\varepsilon}$  is given by  $v_k^N$  for  $k \in J_N$ , where*

$$(v_k^N)_j = e^{2\pi i k \cdot j/n}.$$

The associated eigenvalues  $\lambda_k^{N,\varepsilon}$  satisfy

$$(37) \quad |\lambda_k^{N,\varepsilon} - e^{-\pi^2 \varepsilon |k|^2} \lambda_k| \leq K_d \left( e^{-\frac{1}{8\varepsilon}} + \frac{1 + \varepsilon |k|^2}{n^2 \varepsilon} \right),$$

$$(38) \quad |\lambda_k^{N,\varepsilon}| \leq \frac{K_d}{\varepsilon |k|^2},$$

provided that  $\varepsilon \leq \bar{\varepsilon}_d$  and  $(n^2 \varepsilon)^{-1} \leq \bar{h}_d$ , with positive constants  $K_d$ ,  $\bar{\varepsilon}_d$  and  $\bar{h}_d$  that depend only on the dimension  $d$ . Above, the  $\lambda_k$  are given by (30).

Compared to Proposition 3 we see here the effect of a third length scale  $1/n$ , associated with the discretization. Proposition 4 states that for small  $\varepsilon$ , eigenvalues of  $T^{N,\varepsilon}$  are similar to those of  $T$ , as long as the entropic blur is larger than the discretization scale, but smaller than the scale of the eigenfunction, i.e.

$$\frac{1}{n} \ll \sqrt{\varepsilon} \ll \frac{1}{|k|}.$$

For the torus we will refine this discussion in Section 5.4. More generally, we expect that this observed relation between the three length scales also provides a good intuition for other dynamical systems  $(\mathcal{X}, F, \mu)$ .

*Proof.* To prove that  $v_k^N$  for a given  $k \in J_N$  is an eigenvector, and to calculate its eigenvalue  $\lambda_k^{N,\varepsilon}$ , we need to evaluate at any  $m \in J_N$ :

$$(39) \quad [\Gamma^{N,\varepsilon} v_k^N]_m = \frac{1}{N Z_{N,\varepsilon}} \sum_{\ell \in J_N} e^{-\frac{1}{\varepsilon} d(\ell/n + \theta, m/n)^2} e^{2\pi i k \cdot \ell/n}.$$

By  $n$ -periodicity of both exponents with respect to each component of  $\ell$ , one can shift the domain of summation in  $\mathbb{Z}^d$ . In particular, we may replace the summation over  $\ell \in J_N$  by

$$\ell \in J_{N,\theta} + m \quad \text{where} \quad J_{N,\theta} := \left\{ j \in \mathbb{Z}^d \mid \frac{j}{n} + \theta \in \mathbf{C} \right\}.$$

Notice that  $J_{N,\theta}$  and thus also  $J_{N,\theta} + m$  are indeed translates of  $J_N$ . By definition of  $d$ , we can rewrite (39) as

$$\begin{aligned} [\Gamma^{N,\varepsilon} v_k^N]_m &= \frac{1}{N Z_{N,\varepsilon}} \sum_{\ell \in J_{N,\theta} + m} e^{-\frac{1}{\varepsilon} [(\ell-m)/n + \theta]^2} e^{2\pi i k \cdot \ell/n} \\ &= \frac{1}{N Z_{N,\varepsilon}} \left( \sum_{j \in J_{N,\theta}} e^{-\frac{1}{\varepsilon} [j/n + \theta]^2} e^{2\pi i k \cdot j/n} \right) [v_k^N]_m, \end{aligned}$$

which proves the eigenvector property of  $v_k^N$  with corresponding eigenvalue

$$(40) \quad \lambda_k^{N,\varepsilon} = \frac{1}{N Z_{N,\varepsilon}} \sum_{j \in J_{N,\theta}} e^{-\frac{1}{\varepsilon} [j/n + \theta]^2} e^{2\pi i k \cdot j/n}.$$

We start by proving (37). Directly from (40), recalling that  $\lambda_k = e^{-2\pi i k \cdot \theta}$  by (30), we obtain

$$\begin{aligned} \lambda_k^{N,\varepsilon} &= \frac{\lambda_k}{N Z_{N,\varepsilon}} \sum_{j \in J_{N,\theta}} \exp \left( -\frac{1}{\varepsilon} \left[ \frac{j}{n} + \theta \right]^2 + 2\pi i k \cdot \left( \frac{j}{n} + \theta \right) \right) \\ &= \frac{\lambda_k}{N Z_{N,\varepsilon}} \sum_{j \in J_{N,\theta}} \exp \left( -\left[ \frac{1}{\varepsilon^{1/2}} \left( \frac{j}{n} + \theta \right) - \varepsilon^{1/2} \pi i k \right]^2 \right) e^{-\varepsilon \pi^2 |k|^2}. \end{aligned}$$

For brevity, let

$$(41) \quad \xi_j = \frac{j + n\theta}{n\varepsilon^{1/2}}$$

in the following; then

$$(42) \quad \lambda_k^{N,\varepsilon} = \frac{\lambda_k e^{-\varepsilon\pi^2|k|^2}}{N Z_{N,\varepsilon}} \sum_{j \in J_{N,\theta}} e^{-[\xi_j - \varepsilon^{1/2}\pi ki]^2}, \quad Z_{N,\varepsilon} = \frac{1}{N} \sum_{j \in J_{N,\theta}} e^{-[\xi_j]^2}.$$

To further simplify these expressions, we estimate the errors induced by first replacing the sum over  $j \in J_{N,\theta}$  above by a sum over all  $j \in \mathbb{Z}^d$ , and then by replacing that sum by an integral.

For the passage from  $J_{N,\theta}$  to  $\mathbb{Z}^d$ , we combine two elementary inequalities. Analogous to (33) for  $j \in \mathbb{Z}^d \setminus J_{N,\theta}$ , and for any  $\tau \in \mathbb{R}^d$ ,

$$|e^{-[\xi_j - i\tau]^2}| = e^{|\tau|^2 - |\xi_j|^2} \leq e^{|\tau|^2} e^{-\frac{1}{8\varepsilon}} e^{-\frac{1}{2}|\xi_j|^2},$$

since  $|\xi_j|^2 \geq \frac{1}{4\varepsilon}$ . The second is that for any  $a, b \in \mathbb{R}$  with  $0 < b \leq 1$ ,

$$(43) \quad b \sum_{j \in \mathbb{Z}} e^{-\frac{1}{2}(bj-a)^2} \leq \Theta,$$

with a uniform constant  $\Theta \approx \sqrt{2\pi}$ . Now, assuming that  $n^2\varepsilon \geq 1$  — and setting  $b := (n^2\varepsilon)^{-1/2} \leq 1$  accordingly — we obtain that

$$(44) \quad \frac{1}{N} \left| \sum_{j \in \mathbb{Z}^d} e^{-[\xi_j - i\tau]^2} - \sum_{j \in J_{N,\theta}} e^{-[\xi_j - i\tau]^2} \right| \leq \varepsilon^{d/2} e^{|\tau|^2} e^{-\frac{1}{8\varepsilon}} \prod_{\alpha=1}^d \left( \frac{1}{n\varepsilon^{1/2}} \sum_{j_\alpha \in \mathbb{Z}} e^{-\frac{1}{2}(\frac{j_\alpha}{n\varepsilon^{1/2}} + \theta_\alpha)^2} \right) \leq \varepsilon^{d/2} \Theta^d e^{|\tau|^2} e^{-\frac{1}{8\varepsilon}}.$$

For the passage from the sum to the integral, we use that (41) with  $j \in \mathbb{Z}^d$  arbitrary defines a  $d$ -dimensional uniform lattice in  $\mathbb{R}^d$  of mesh size  $(n^2\varepsilon)^{-1/2}$ . We associate each  $j \in \mathbb{Z}^d$  to the half-open cube

$$B_j := \xi_j + (n^2\varepsilon)^{-1/2}\mathbf{C}.$$

The  $B_j$  form a tessellation of  $\mathbb{R}^d$ . A second order Taylor expansion of an arbitrary  $C^2$ -function  $h : \mathbb{R}^d \rightarrow \mathbb{R}$  around  $\xi_j$  yields:

$$\left| \int_{B_j} h(\zeta) d\zeta - h(\xi_j) \right| \leq \frac{d}{24n^2\varepsilon} \sup_z \|\nabla^2 h(z)\|_{\text{op}},$$

where  $\|\nabla^2 h(z)\|_{\text{op}}$  is the Euclidean operator norm of the matrix  $\nabla^2 h(z)$ . For  $h(z) = e^{-[z - i\tau]^2}$ , we have

$$\nabla^2 h(z) = h(z) \left( (4zz^T - 4\tau\tau^T - 2\text{id}) - 4i(\tau z^T + z\tau^T) \right),$$

and therefore, observing that  $(1+u)e^{-u/2} \leq 2$  for all real  $u$ ,

$$\begin{aligned} \|\nabla^2 h(z)\|_{\text{op}} &\leq (\|4zz^T - 4\tau\tau^T - 2\text{id}\|_{\text{op}} + 4\|\tau z^T + z\tau^T\|_{\text{op}})|h(z)| \\ &\leq (2 + 4|z|^2 + 4|\tau|^2 + 8|\tau||z|)e^{|\tau|^2 - |z|^2} \\ &\leq 8(1 + |\tau|^2)e^{|\tau|^2}(1 + |z|^2)e^{-\frac{1}{2}|z|^2}e^{-\frac{1}{2}|z|^2} \leq 16(1 + |\tau|^2)e^{|\tau|^2}e^{-\frac{1}{2}|z|^2}. \end{aligned}$$

Hence, the difference between  $h$ 's integral and its approximation by sums can be estimated as follows:

$$(45) \quad \left| \int_{\mathbb{R}^d} e^{-[\xi - i\tau]^2} d\xi - (n^2\varepsilon)^{-d/2} \sum_{j \in \mathbb{Z}^d} e^{-[\xi_j - i\tau]^2} \right| \leq \frac{16d(1 + |\tau|^2)e^{|\tau|^2}}{24n^2\varepsilon} (n^2\varepsilon)^{-d/2} \sum_{j \in \mathbb{Z}^d} e^{-\frac{1}{2}|\xi_j|^2} \\ \leq \frac{2d\Theta^d}{3} \cdot \frac{(1 + |\tau|^2)e^{|\tau|^2}}{n^2\varepsilon}.$$

Now recall that by (34), the value of the integral above is  $\pi^{d/2}$ , independently of  $\tau$ . We combine the estimates (44) and (45) and apply them to the representations of  $\lambda_k^{N,\varepsilon}$  and of  $Z^{N,\varepsilon}$  in (42), with  $\tau = 0$  and  $\tau = \sqrt{\varepsilon}\pi k$ , respectively. This yields:

$$(46) \quad \left| \pi^{d/2} - \varepsilon^{-d/2} Z^{N,\varepsilon} \right| \leq \Theta^d \left( e^{-\frac{1}{8\varepsilon}} + \frac{2d}{3n^2\varepsilon} \right),$$

$$(47) \quad \left| \pi^{d/2} \lambda_k - e^{\varepsilon\pi^2|k|^2} \varepsilon^{-d/2} Z_{N,\varepsilon} \lambda_k^{N,\varepsilon} \right| \leq \Theta^d e^{\varepsilon\pi^2|k|^2} \left( e^{-\frac{1}{8\varepsilon}} + \frac{2d(1 + \varepsilon\pi^2|k|^2)}{3n^2\varepsilon} \right).$$

Finally, we assume that  $\varepsilon > 0$  is sufficiently small and  $n$  is (in dependence on  $\varepsilon$ ) sufficiently large so that

$$(48) \quad \Theta^d \left( e^{-\frac{1}{8\varepsilon}} + \frac{2d}{3n^2\varepsilon} \right) \leq \frac{\pi^{d/2}}{2}, \quad \text{and consequently} \quad \varepsilon^{-d/2} Z^{N,\varepsilon} \geq \frac{\pi^{d/2}}{2}.$$

The claim (37) is now proven simply combining (46), (47) and (48):

$$\begin{aligned} |\lambda_k^{N,\varepsilon} - e^{-\pi^2\varepsilon|k|^2} \lambda_k| &= \frac{\varepsilon^{d/2} e^{-\pi^2\varepsilon|k|^2}}{Z_{N,\varepsilon}} (|e^{\pi^2\varepsilon|k|^2} \varepsilon^{-d/2} Z_{N,\varepsilon} \lambda_k^{N,\varepsilon} - \varepsilon^{-d/2} Z_{N,\varepsilon} \lambda_k|) \\ &\leq \frac{\varepsilon^{d/2} e^{-\pi^2\varepsilon|k|^2}}{Z_{N,\varepsilon}} (|e^{\pi^2\varepsilon|k|^2} \varepsilon^{-d/2} Z_{N,\varepsilon} \lambda_k^{N,\varepsilon} - \lambda_k \pi^{d/2}| + |\pi^{d/2} - \varepsilon^{-d/2} Z_{N,\varepsilon}|) \\ &\leq \frac{2(1 + e^{-\pi^2\varepsilon|k|^2})\Theta^d}{\pi^{d/2}} \left( e^{-\frac{1}{8\varepsilon}} + \frac{2d(1 + \varepsilon\pi^2|k|^2)}{3n^2\varepsilon} \right). \end{aligned}$$

We turn to the proof of (38). Assume  $k \in J_N$  is not zero. Without loss of generality, let  $k_1$  be a component with largest modulus, i.e.,  $|k|^2 \leq dk_1^2$ . We write  $k = (k_1, k')$  and decompose  $j \in J_N$  accordingly as  $j = (j_1, j') \in J \times J'$ , as well as  $\theta = (\theta_1, \theta')$ . We then have, with the

obvious adaptation of notations,

$$(49) \quad \begin{aligned} |N Z_{N,\varepsilon} \lambda_k^{N,\varepsilon}| &= \left| \sum_{(j_1, j') \in J_N} e^{-\frac{1}{\varepsilon}[j'/n + \theta']^2} e^{2\pi i k' \cdot j'/n} e^{-\frac{1}{\varepsilon}(j_1/n + \theta_1)^2} e^{2\pi i k_1 j_1/n} \right| \\ &\leq \sum_{j' \in J'} e^{-\frac{1}{\varepsilon}[j'/n + \theta']^2} I, \text{ where } I := \left| \sum_{j_1 \in J} e^{-\frac{1}{\varepsilon}(j_1/n + \theta_1)^2} e^{2\pi i k_1 j_1/n} \right|. \end{aligned}$$

To estimate  $I$  further, we perform a summation by parts: for any complex numbers  $a_\ell, b_\ell$ , one has that

$$(50) \quad \begin{aligned} \sum_{\ell=L^-}^{L^+} b_\ell (a_{\ell+1} - 2a_\ell + a_{\ell-1}) &= \sum_{\ell=L^-}^{L^+} (b_{\ell+1} - 2b_\ell + b_{\ell-1}) a_\ell \\ &\quad + a_{L^+} b_{L^+} - a_{L^+} b_{L^+} + a_{L^-} b_{L^-} - a_{L^-} b_{L^-}. \end{aligned}$$

We substitute

$$e^{2\pi i k_1 j_1/n} = -\frac{e^{2\pi i k_1 (j_1+1)/n} - 2e^{2\pi i k_1 j_1/n} + e^{2\pi i k_1 (j_1-1)/n}}{2(1 - \cos(2\pi k_1/n))},$$

and use (50):

$$(51) \quad \begin{aligned} &2(1 - \cos(2\pi k_1/n))I \\ &= \left| \sum_{j_1 \in J} e^{-\frac{1}{\varepsilon}(j_1/n + \theta_1)^2} (e^{2\pi i k_1 (j_1+1)/n} - 2e^{2\pi i k_1 j_1/n} + e^{2\pi i k_1 (j_1-1)/n}) \right| \\ &= \left| \sum_{j_1 \in J} (e^{-\frac{1}{\varepsilon}((j_1+1)/n + \theta_1)^2} - 2e^{-\frac{1}{\varepsilon}(j_1/n + \theta_1)^2} + e^{-\frac{1}{\varepsilon}((j_1-1)/n + \theta_1)^2}) e^{2\pi i k_1 j_1/n} + B \right| \\ &= \left| \frac{1}{n^2} \sum_{j_1 \in J} \left( 4 \left( \frac{\nu_{j_1} + \theta_1}{\varepsilon} \right)^2 - \frac{2}{\varepsilon} \right) e^{-\frac{1}{\varepsilon}(\nu_{j_1} + \theta_1)^2} + B \right| \\ &\leq \frac{1}{n^2 \varepsilon} \sum_{j_1 \in J} \left( 4 \left( \frac{\nu_{j_1} + \theta_1}{\sqrt{\varepsilon}} \right)^2 + 2 \right) \exp \left( - \left( \frac{\nu_{j_1} + \theta_1}{\sqrt{\varepsilon}} \right)^2 \right) + |B|. \end{aligned}$$

Here  $\nu_{j_1}$  is a suitable intermediate value between  $(j_1 - 1)/n$  and  $(j_1 + 1)/n$ , provided by Taylor's theorem, and  $B$  summarizes the ‘‘boundary terms’’; according to (50),  $B$  is the sum of four products of the form

$$\pm e^{-\frac{1}{\varepsilon}(j_1/n + \theta_1)^2} e^{2\pi i k_1 j_1/n}$$

with  $|j_1/n + \theta_1| \geq 1/2 - 1/n \geq 1/4$ , and thus

$$|B| \leq 4e^{-1/(16\varepsilon)}.$$

Next, consider  $J_+ \subset J$  containing all  $j_1 \in J$  with  $\nu_{j_1} + \theta_1 \geq 0$ . Further, let  $n^* \in \mathbb{Z}$  be the smallest index greater than  $n\sqrt{\varepsilon}$ . Since we are interested in large  $n\sqrt{\varepsilon}$ , it is not restrictive to assume that

$$\sigma_{j_1} := \frac{\nu_{j_1} - (j_1 - n^*)/n}{\sqrt{\varepsilon}} \in \left[ \frac{n^* - 1}{n\sqrt{\varepsilon}}, \frac{n^* + 1}{n\sqrt{\varepsilon}} \right] \subset [1/2, 2]$$

for all  $j_1 \in J_+$ . With  $\eta_{j_1} := \frac{\nu_{j_1} + \theta_1}{\sqrt{\varepsilon}} \geq 0$ , it is elementary to verify that

$$(52) \quad (4\eta_{j_1}^2 + 2)e^{-\eta_{j_1}^2} \leq 8e^4 e^{-(\eta_{j_1} - \sigma_{j_1})^2},$$

which is, more explicitly,

$$\left( 4 \left( \frac{\nu_{j_1} + \theta_1}{\sqrt{\varepsilon}} \right)^2 + 2 \right) \exp \left( - \left( \frac{\nu_{j_1} + \theta_1}{\sqrt{\varepsilon}} \right)^2 \right) \leq 8e^4 \exp \left( - \left( \frac{(j_1 - n^*)/n + \theta_1}{\sqrt{\varepsilon}} \right)^2 \right).$$

Provided that  $\varepsilon < 1/4$  and thus  $n^*/n < 1/2$ , it follows that  $j_1 - n^* \in J$  for all  $j_1 \in J_+$ , and therefore, by a simple index shift,

$$\sum_{j_1 \in J_+} \left( 4 \left( \frac{\nu_{j_1} + \theta_1}{\sqrt{\varepsilon}} \right)^2 + 2 \right) \exp \left( - \left( \frac{\nu_{j_1} + \theta_1}{\sqrt{\varepsilon}} \right)^2 \right) \leq 8e^4 \sum_{j_1 \in J} e^{-\frac{1}{\varepsilon}(j_1/n + \theta_1)^2}.$$

An analogous reasoning applies to the set  $J_-$  of indices  $j_1 \in J$  with  $\nu_{j_1} + \theta_1 < 0$  in place of  $J_+$ . Recalling (51), we conclude that

$$I \leq \frac{C}{n^2 \varepsilon (1 - \cos(2\pi k_1/n))} \sum_{j_1 \in J} e^{-\frac{1}{\varepsilon}(j_1/n + \theta_1)^2} + 4e^{-1/(16\varepsilon)},$$

for some universal constant  $C$ . In combination with the elementary estimate  $\cos t \leq 1 - \frac{1}{8}t^2$  for all  $|t| \leq \pi$ , and by increasing the value of  $C$  to accommodate the term  $4e^{-1/(16\varepsilon)}$ , we obtain from (49) that

$$|N Z_{N,\varepsilon} \lambda_k^{N,\varepsilon}| \leq \frac{C}{\varepsilon |k_1|^2} \sum_{j' \in J'} e^{-\frac{1}{\varepsilon}[j'/n + \theta']^2} \sum_{j_1 \in J} e^{-\frac{1}{\varepsilon}(j_1/n + \theta_1)^2} \leq \frac{dCN Z_N}{\varepsilon |k|^2},$$

which shows (38).  $\square$

**5.4. Consequence: accumulation of eigenvalues.** In this section, we draw several conclusions from Propositions 3 and 4 on the relation between the shift  $\theta$ , the length scales  $\varepsilon^{1/2}$  and  $n^{-1}$ , and the accumulation of eigenvalues  $\lambda_k^{N,\varepsilon}$  on or near the unit circle. The goal is to give a theoretically founded explanation for some of the results from numerical experiments that are presented in Section 6.1 further below and to provide some intuition for more general systems.

We start by discussing the smallness assumption  $n^{-1} \ll \sqrt{\varepsilon}$  of Proposition 4. This is far more than a technical hypothesis: we claim that, generically, the discretized dynamics does need a blur that stretches over several cells of the discretization in order to produce meaningful results.

Indeed, writing in the representation (40) of  $\lambda_k^{N,\varepsilon}$  the exponent as  $[j + n\theta]^2/(n^2\varepsilon)$ , it is easily seen that for  $n^2\varepsilon$  of order one or less, the entire sum reduces essentially to only one term, namely the one for the index  $\bar{m} \in J_{N,\theta}$  closest to  $-n\theta$ . Consequently,  $\lambda_k^{N,\varepsilon} \approx e^{2\pi i k \cdot \bar{m}/n}$  for all  $k$ . That is, a large portion of the  $N$  eigenvalues lies very close to the unit circle, in groups with uniform angular distance. This is very little and structurally highly unstable information.

For illustration, consider  $d = 1$  dimensions with  $\theta = 1/11$ : the spectrum of the pure transfer operator  $T$  consists of eleven equally spaced groups of eigenvalues on the unit circle. For discretizations with  $n = 10$ ,  $n = 100$ ,  $n = 1000$  etc. points, we find that the limiting spectrum always consists of  $n$  groups of points (since the integer  $\bar{m}$  nearest to  $-n/11$  never has two or five as prime factor). Hence the coarsest discretization with  $n = 10$  produces the qualitatively best approximation, the additional structures that appear in the finer discretizations are only misleading.

Therefore, we shall assume  $n^{-1} \ll \sqrt{\varepsilon}$  from now on. Under this hypothesis, estimate (37) implies a good agreement between the genuine eigenvalues  $\lambda_k^{N,\varepsilon}$  and their  $N$ -independent approximations

$$\Lambda_k^\varepsilon := e^{-\varepsilon\pi^2|k|^2} e^{-2\pi i k \cdot \theta},$$

at least for sufficiently small indices  $k$ , that is  $|k|^{-1} \ll \sqrt{\varepsilon}$ . Actually, for larger  $|k|$ , the respective eigenvalues  $\lambda_k^{N,\varepsilon}$  lie close to the origin thanks to (38), and provide no significant information. Since we are interested in the spectrum close to the unit circle, it is sufficient to study the  $\Lambda_k^\varepsilon$  with small  $k$  in the sense above.

For ease of presentation, let  $d = 1$ , so that  $\theta \in (-1/2, 1/2)$  is a real number. Assume that  $p, q \in \mathbb{Z}$  are co-prime integers with  $q > 0$  such that

$$(53) \quad \delta := \theta - \frac{p}{q} \quad \text{satisfies} \quad c := q^2|\delta| \in (0, 1).$$

Notice that by Dirichlet's approximation theorem, there are infinitely many such pairs  $(p, q)$  for each irrational  $\theta$ . The smaller  $c$  is, the more pronounced is the accumulation phenomenon described below.

Define the index set  $L_q := \{k \in \mathbb{Z} : -q < 2k \leq q\}$ . The  $q$  points  $\Lambda_k^\varepsilon$  for  $k \in L_q$  have almost uniform angular distance of  $2\pi/q$ . Actually,

$$\frac{\Lambda_k^\varepsilon}{|\Lambda_k^\varepsilon|} = e^{-2\pi i k(p/q + \delta)} = e^{-2\pi i k p/q} e^{i\phi},$$

with  $|\phi| = |2\pi k \delta| \leq \pi q \delta < \pi/q$  by (53), so that the variation of the individual angular positions is less than half of the expected angular distance  $2\pi/q$ . An analogous argument applies also to the shifted index sets  $L_q + mq$  with an arbitrary  $m \in \mathbb{Z}$ ; the corresponding  $\Lambda_k^\varepsilon$  form a group of  $q$  points with approximately uniform angular distance of  $2\pi/q$ . Notice that the smaller  $c \in (0, 1)$ , the more uniform the angles between the  $\Lambda_k^\varepsilon$  in each group  $k \in L_q + mq$ , and the better the alignment of two different such groups with similar  $m$ .

Are these groups visible in the spectrum of  $T^{N,\varepsilon}$ ? If  $q \gg \varepsilon^{-1/2}$ , then estimate (37) fails, and the positions of the approximations  $\Lambda_k^\varepsilon$  gives little information on the positions

of the genuine eigenvalues  $\lambda_k^{N,\varepsilon}$ . If, on the other hand,  $q \ll \varepsilon^{-1/2}$ , then the modulus  $|\Lambda_k^\varepsilon| = e^{-\pi\varepsilon k^2}$  is approximately one for  $k$ 's from several different groups  $L_q + mq$ . Thus, there will be significantly more than  $q$  points close to the unit circle, and the groups difficult to distinguish.

The most interesting regime is thus if  $q$  is of the order of  $\varepsilon^{-1/2}$ . Then the moduli of the  $q$  points  $\Lambda_k^\varepsilon$  in one group  $k \in L_q + mq$  are still comparable, but the difference between corresponding points in two consecutive groups with  $k \in L_q + mq$  and with  $k \in L_q + (m+1)q$ , respectively, are notable — there is at least a factor of  $e^{-\pi\varepsilon q^2}$ . In particular, there is one distinguished group of eigenvalues very close to the unit circle, namely for  $k \in L_q$ , and that one is accompanied by pairs of groups of  $\Lambda_k^{N,\varepsilon}$  with  $k \in L_q \pm mq$  for  $m = 1, 2, 3, \dots$  that are moving successively closer to the origin as  $m$  increases.

For a specific example, let  $n = 1000$ ,  $\theta = 1/\pi$ . The best three rational approximations  $p/q$  of  $\theta$  — in the sense of smallest  $c$  in (53) — with  $q < n$  are given by

$$(p, q) \in \{(1, 3), (7, 22), (113, 355)\},$$

with corresponding values for  $c$ :

$$c_{(1,3)} = 0.135\dots, \quad c_{(7,22)} = 0.062\dots, \quad c_{(113,355)} = 0.003\dots$$

The constant  $c$  attains exceptionally small values in this example; this is due to the number theoretic properties of  $\pi$ .

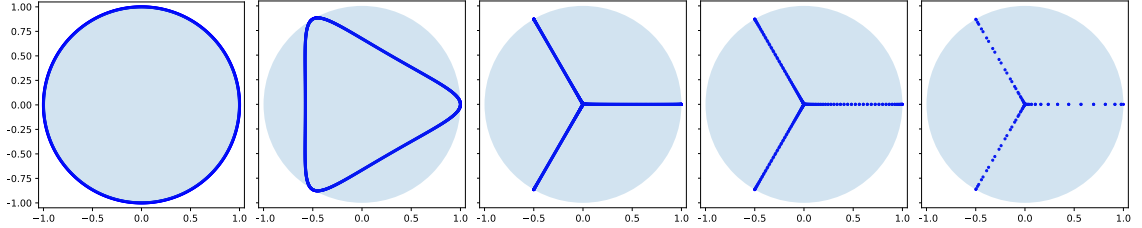
The corresponding approximate 355-, 22-, and 3-cycles should be visible approximately up to  $\varepsilon \lesssim (\pi \cdot 355)^{-2} \approx 8 \cdot 10^{-7}$ ,  $\varepsilon \lesssim 2 \cdot 10^{-4}$  and  $\varepsilon \lesssim 10^{-2}$  respectively. For  $\varepsilon \lesssim 1/n^2 = 10^{-6}$  we expect visible discretization artifacts in the spectrum, i.e. the 355-cycle will already be hidden by discretization. The other two should become subsequently apparent as  $\varepsilon$  is gradually increased towards 1. This intuition will be confirmed in the numerical examples, see Figure 4.

## 6. NUMERICAL EXPERIMENTS

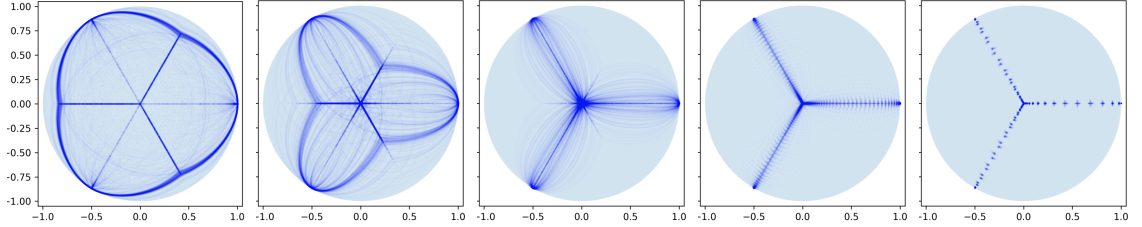
The following numerical experiments have been carried out in the Python programming language, partially using the KeOps package [7] which allows for an efficient and stable implementation of the Sinkhorn algorithm. The corresponding scripts are available at <https://github.com/gaioguy/EntropicTransferOperators>.

**6.1. The shift map on the circle.** As a first numerical test we consider the shift map from Section 5 on the circle  $\mathcal{X} = S^1 = \mathbb{R}/\mathbb{Z}$ . We examine the case of rational  $\theta = \frac{1}{3}$  first, i.e. such that the circle decomposes into three subsets which are cyclically permuted by  $F$ . Correspondingly, we expect the spectrum of  $\Gamma^{N,\varepsilon}$  to exhibit the 3rd roots of unity. Indeed, the spectra shown in Figure 3 clearly show these - expect for  $\varepsilon = 10^{-6}$  and using a lattice as the underlying discretization. In fact, in this case  $\Gamma^{N,\varepsilon}$  turns out to be a permutation matrix. This is in agreement with the discussion of Section 5.4 as  $n = 1000$  and 3 are coprime.

For irrational  $\theta = \frac{1}{\pi} \approx \frac{1}{3}$  the spectra that we obtain experimentally are shown in Figure 4. As expected, with increasing  $\varepsilon$  they are in excellent agreement with the asymptotics given



(A) Points on a lattice.



(B) Random points: histogram of the spectra of 100 realisations.

FIGURE 3. Circle shift with  $\theta = \frac{1}{3}$  using  $N = 1000$  points: spectra of  $\Gamma^{N,\varepsilon}$  for  $\varepsilon$  from  $10^{-6}$  to  $10^{-2}$  (left to right)

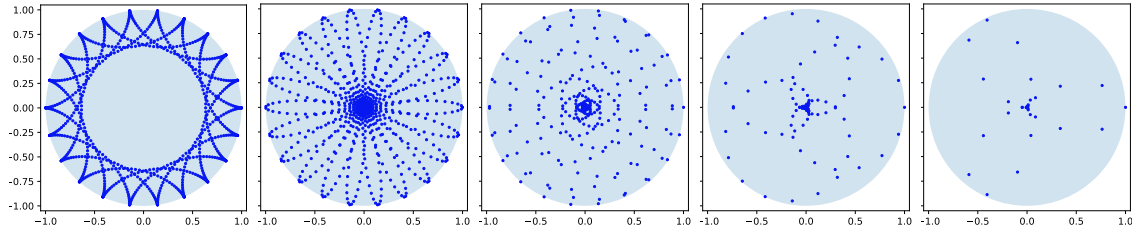
by Proposition 3. The map does not exhibit an exact macroscopic three cycle. However, in accordance with the discussion of Section 5.4, it exhibits approximate  $q$ -cycles for various  $q$ , in particular for  $q = 22$  and  $q = 3$  and these are visible in the corresponding regimes of  $\varepsilon$ .

In Section 5 the discretization of  $\mathcal{X}$  was uniform as it allowed an analytic (approximate) treatment of the system by leveraging the high level of symmetry. The convergence results of Section 4 do not require such regularity. This is confirmed by Figures 3b and 4b, where histograms of the spectra of  $\Gamma^{N,\varepsilon}$  are shown for 100 realizations of a random choice of the underlying point cloud (i.e. each point  $x_j$  is chosen independently from a uniform distribution on  $S^1$ ). The results are robust and consistent. This implies that our method can be used reliably on a wide variety of input data  $\mu^N$ .

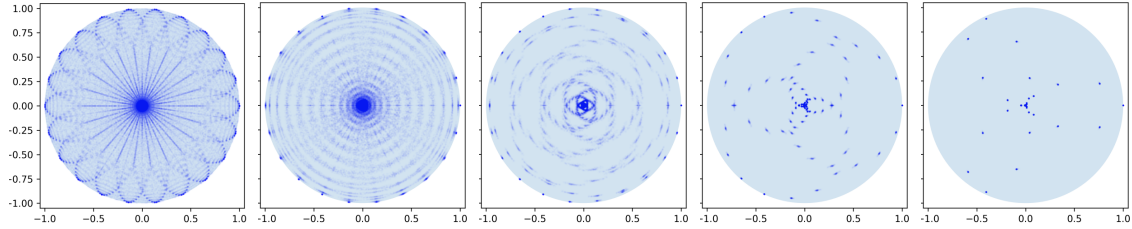
**6.2. The Lorenz system.** For a second experiment, we consider the classical Lorenz system [19]

$$\begin{aligned}\dot{u} &= \sigma(v - u) \\ \dot{v} &= u(\rho - w) - v \\ \dot{w} &= uv - \beta w\end{aligned}$$

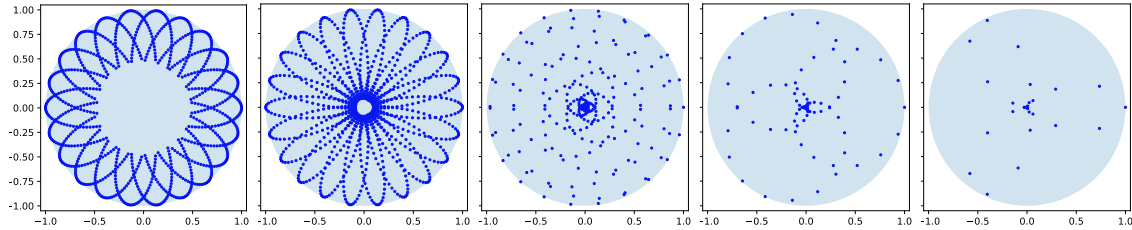
with parameter values  $\sigma = 10, \rho = 28, \beta = 8/3$ . The system possesses a robust strange attractor [26] which can be decomposed into several almost invariant sets [12]. We approximate the attractor by a point cloud  $x_1, \dots, x_N$  ( $N = 2000$  and  $N = 4000$ ) resulting from



(A) Points on a lattice.



(B) Random points: histogram of the spectra of 100 realisations.

(C) Eigenvalue asymptotics from Proposition 3,  $\varepsilon$  from  $3 \cdot 10^{-7}$  to  $3 \cdot 10^{-3}$  (left to right).FIGURE 4. Circle shift with  $\theta = \frac{1}{\pi}$  using  $N = 1000$  points: spectra of  $\Gamma^{N,\varepsilon}$  for  $\varepsilon$  from  $10^{-5}$  to  $10^{-1}$  (left to right).

an equidistant sampling of the trajectory  $X = (u, v, w) : [0, 800] \rightarrow \mathbb{R}^3$  with initial value  $X(0) = (1, 1, 1)$ . The map  $F$  is given by the time-0.1 flow map of the system.

The real spectra of  $\Gamma^{N,\varepsilon}$  close to 1 in dependence of  $\varepsilon$  are shown in Fig. 5. For both sampling densities, there are two real eigenvalues  $\lambda_1, \lambda_2 < 1$  which decay much slower with  $\varepsilon$  increasing from 0.01 to 1 than the other eigenvalues. The corresponding eigenvectors each give rise to a decomposition of the point cloud into two almost invariant sets via their sign structure as shown in Fig. 6 (left and center), cf. [10, 12]. For  $N = 2000$  points, there is also a third eigenvalue  $\lambda_3$  very close to 1 one which quickly decays away from 1 at  $\varepsilon \approx 1$ . It corresponds to a point  $x_i$  near the origin where the point density is low and  $F(x_i) \approx x_i$ , such that for sufficiently small  $\varepsilon$ , mass at  $F(x_i)$  gets transported almost exclusively back to  $x_i$ , thus forming a spurious invariant set that decays quickly as  $\sqrt{\varepsilon}$  reaches the scale of nearest neighbor distances around  $x_i$ . Such isolated points become less likely as  $N$  is increased and their eigenvectors can be identified easily.

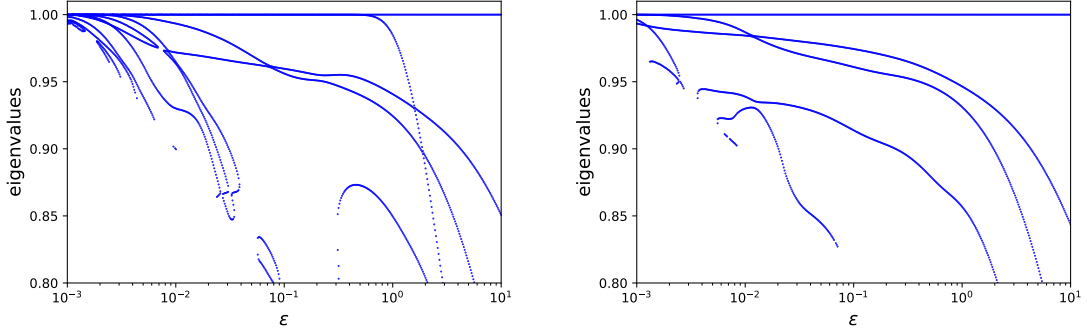


FIGURE 5. Lorenz system: largest real eigenvalues of  $\Gamma^{N,\varepsilon}$  in dependence of  $\varepsilon$  for  $N = 2000$  (left) and  $N = 4000$  (right) points.

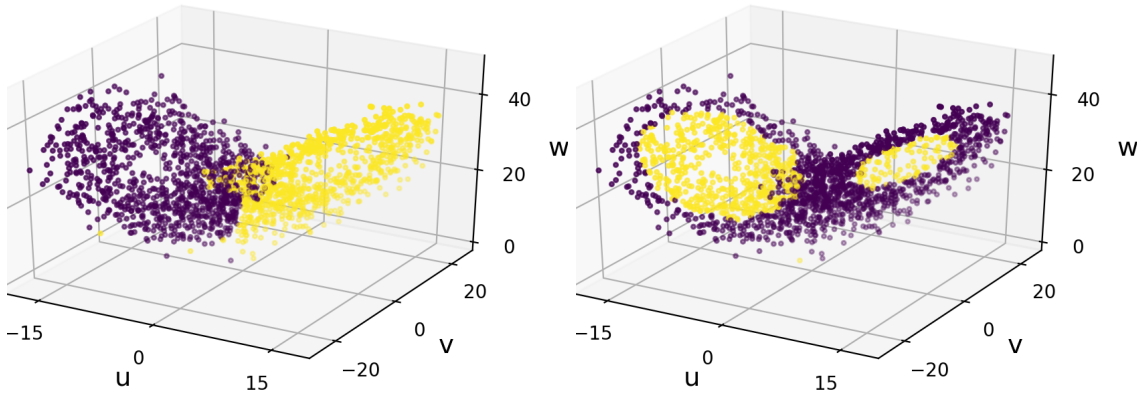


FIGURE 6. Lorenz system: eigenvectors at  $\lambda_1 \approx 0.94$  (left),  $\lambda_2 \approx 0.92$  (right) of  $\Gamma^{N,\varepsilon}$  for  $\varepsilon = 1.0$  according to their signs.

**6.3. Alanine dipeptide.** As a third experiment we analyse the dynamics of alanine dipeptide, a small biomolecule which is often used as a non-trivial model system for the analysis of macroscopic dynamics, cf. for example [16]. Like in the Lorenz system, we use trajectory data, here on the positions of the heavy atoms as provided by [23, 29]<sup>4</sup>. The original time series results from time integration of the molecule over 250ns with a time step of 1ps, yielding  $M = 250\,000$  points  $\hat{x}_1, \dots, \hat{x}_M$  in  $\mathbb{R}^{30}$ . Here, we subsample this trajectory and use only every 50th (resp. 25th) point, yielding a sequence  $x_1, \dots, x_N$ ,  $N = 5\,000$  (resp. 10\,000), in  $\mathbb{R}^{30}$  which forms the data for our analysis. We define the map  $F$  by time-delay, that is we let  $F(\hat{x}_j) := \hat{x}_{j+10}$  for  $j = 1, \dots, M - 10$ . This time lag of 10 ps has been chosen experimentally such that the real spectrum of  $\Gamma^{N,\varepsilon}$  is reasonably close to 1. We

<sup>4</sup>The data is available for download at <https://markovmodel.github.io/mdshare/ALA2/>.

note, however, that the macroscopic structure of the eigenvectors, cf. Fig. 9, remains the same for time lags between 1 ps and 30 ps (while, of course, the spectrum changes).

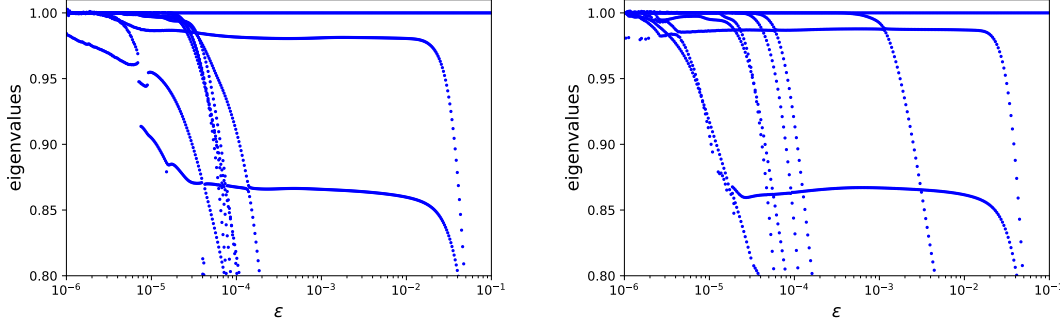


FIGURE 7. Alanine dipeptide: largest real eigenvalues of  $\Gamma^{N,\varepsilon}$  in dependence of  $\varepsilon$  for  $N = 5000$  (left) and  $N = 10000$  samples (right).

Figure 7 (left) shows the dominant real spectrum of  $\Gamma^{N,\varepsilon}$  close to 1 in dependence of  $\varepsilon$  for both sampling densities. There appear to be two eigenvalues  $\lambda_1 \approx 0.98$  and  $\lambda_2 \approx 0.87$  which are essentially constant over several orders of magnitude of  $\varepsilon$ . In fact, the corresponding eigenvectors (cf. Fig. 7) give rise to the decomposition of the point cloud into three almost invariant sets as shown in Fig. 9, see below. Additionally, for small  $\varepsilon$ , there are several eigenvalues very close to one which decay away from 1 for, in comparison to  $\lambda_1$  and  $\lambda_2$ , small values of  $\varepsilon$ . These seem to correspond to spurious invariant subsets of point cloud.

In order to better understand the behaviour of the eigenvalues with increasing  $\varepsilon$ , we consider the simple Markov chain model with three states shown in Fig. 8. We assume that the distance  $d_1$  between the states 2 and 3 is much (i.e. an order of magnitude) smaller than the distance  $d_2$  between 1 and 2 resp. 3. The transition matrix for this Markov chain is given by

$$T = \begin{bmatrix} 1 - 2p_2 & p_2 & p_2 \\ p_2 & 1 - p_1 - p_2 & p_1 \\ p_2 & p_1 & 1 - p_1 - p_2 \end{bmatrix}.$$

Let  $G^\varepsilon \in \mathbb{R}^{3 \times 3}$  denote the matrix of the entropically regularized transport plan for the associated distance matrix

$$\begin{bmatrix} 0 & d_2 & d_2 \\ d_2 & 0 & d_1 \\ d_2 & d_1 & 0 \end{bmatrix},$$

so that the entropically smoothed transfer operator is represented by the matrix  $\Gamma^\varepsilon = G^\varepsilon T$ . There are two realms for  $\varepsilon$  for which the eigenvalues of  $\Gamma^\varepsilon$  are essentially constant: For  $\varepsilon \ll d_2^2$ , the smoothing has essentially no effect and the spectrum of  $\Gamma^\varepsilon$  approximately coincides with that of  $T$  itself. For  $\varepsilon \approx d_2^2$ , the smoothing starts to have an effect on the  $2 \leftrightarrow 3$  transition so that the associated eigenvalue starts to drop. At  $\varepsilon \approx d_1^2$ , also the

$1 \leftrightarrow \{2, 3\}$  transition is affected and the second real eigenvalue close to 1 starts to drop as well.

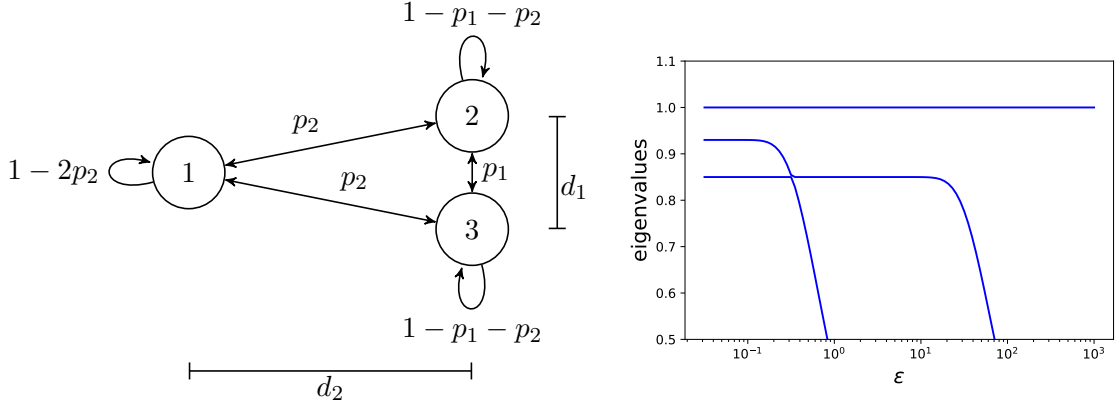


FIGURE 8. Simple Markov model showing the qualitative behaviour of the spectrum in Fig. 7 for  $p_1 = 0.01$ ,  $p_2 = 0.05$ ,  $d_1 = 1$ ,  $d_2 = 10$ .

Let us now return to the alanine dipeptide molecule. In Figure 9, we show the eigenvectors at  $\lambda_1 \approx 0.98$  and  $\lambda_2 \approx 0.86$  for different values of  $\varepsilon$ , projected onto the two relevant dihedral angles of the molecule. A kmeans-clustering of these (for  $\varepsilon = 0.01$ ) yields the three almost invariant (metastable) sets shown in Fig. 10 which correspond to the well-known dominant conformations of the molecule, cf. [16]. We stress the fact that we do not use any prior information on the dihedral angles in the computation but merely the raw trajectory data as described above. The angles are only used for the visualization of the eigenfunctions.

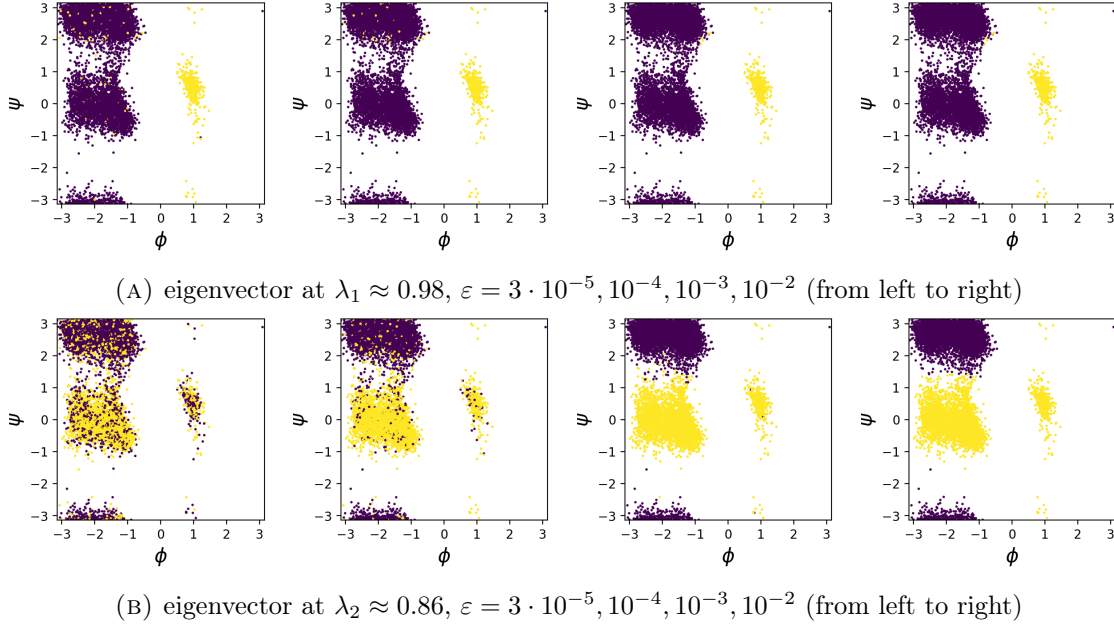


FIGURE 9. Alanine dipeptide: eigenvectors at the dominant two real eigenvalues  $< 1$  of  $\Gamma^{N,\varepsilon}$  according to their signs, projections onto the two dihedral angles.

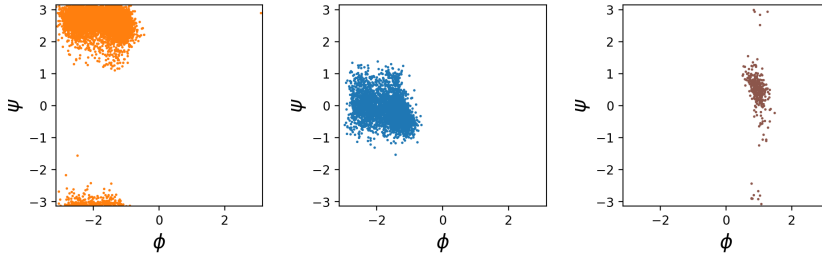


FIGURE 10. Alanine dipeptide: almost invariant sets as resulting from a kmeans-clustering of the two dominant eigenvectors at  $\varepsilon = 0.01$ , projections onto the two dihedral angles.

## 7. CONCLUSION

In this article we have introduced a new method for the discretization and numerical spectral analysis of transfer operators by regularization with entropic optimal transport. The analysis of the torus shift map and the numerical experiments indicate that this might be a promising avenue to follow.

Due to its Lagrangian nature, the method is readily applicable to problems with high-dimensional dynamics, in contrast to grid or set oriented methods, since no explicit covering of the support of the invariant measure  $\mu$  needs to be constructed. Still, as always, the usefulness and/or validity of the numerical results will depend on how well a given discretization is able to capture the macroscopic features of interest. The results in Section 5 give a first impression on how “feature size”, discretization scale and blur scale may be intertwined. Clearly, features below the blur scale will not be uncovered. On the other hand the blur scale needs to be above the discretization scale since otherwise the discrete transfer operator approximation degenerates to a permutation matrix.

A better analytical understanding between the three scales beyond the shift map on the torus would therefore be a relevant open question. For example, the invariant measure in the torus example has full support and thus the required relation between  $N$  and  $\varepsilon$  was given by  $N = n^d \gg \varepsilon^{-d/2}$ , i.e. the required number of points to resolve a given blur scale increases exponentially with  $d$ , the so-called curse of dimensionality. In other cases, when the dimension of the support of  $\mu$  is lower than the dimension of  $\mathcal{X}$ , it seems plausible that  $N$  scales based on the dimension of the former, not the latter, as suggested by the alanine dipeptide example in  $d = 30$ . Can this be established rigorously? See [22] for a related result. When only a low  $N$  is available, can we still expect to reliably recover features at least on coarse scales? These questions may be related to the improved sample complexity of entropic optimal transport as compared to the unregularized version [13]. Such results would confirm that our method can extract some spectral information even from coarse approximations of  $\mu$ , as indicated by some of the numerical experiments.

While here we formulated our approach for an underlying deterministic map, an application to a stochastic model is straightforward: The original transfer operator  $T$  will then be defined in directly terms of a stochastic transition function (instead of constructing it from some deterministic  $F$ ), the rest of the construction remains the same. In fact, computationally a single realization of some random trajectory of the stochastic model might already be sufficient, if it samples the support of the invariant measure well enough.

## REFERENCES

- [1] L. Ambrosio, N. Gigli, and G. Savaré. *Gradient Flows in Metric Spaces and in the Space of Probability Measures*. Lectures in Mathematics. Birkhäuser Boston, 2nd edition, 2008.
- [2] C. Bose and R. Murray. The exact rate of approximation in Ulam’s method. *Discrete Contin. Dynam. Systems*, 7(1):219–235, 2001.
- [3] J. H. Bramble and J. Osborn. Rate of convergence estimates for nonselfadjoint eigenvalue approximations. *Mathematics of computation*, 27(123):525–549, 1973.
- [4] Y. Brenier. Polar factorization and monotone rearrangement of vector-valued functions. *Comm. Pure Appl. Math.*, 44(4):375–417, 1991.
- [5] T. Cai, J. Cheng, B. Schmitzer, and M. Thorpe. The linearized Hellinger–Kantorovich distance. *SIAM J. Imaging Sci.*, 15(1):45–83, 2022.
- [6] G. Carlier, V. Duval, G. Peyré, and B. Schmitzer. Convergence of entropic schemes for optimal transport and gradient flows. *SIAM J. Math. Anal.*, 49(2):1385–1418, 2017.
- [7] B. Charlier, J. Feydy, J. A. Glaunès, F.-D. Collin, and G. Durif. Kernel operations on the GPU, with autodiff, without memory overflows. *Journal of Machine Learning Research*, 22(74):1–6, 2021.

- [8] M. Cuturi. Sinkhorn distances: Lightspeed computation of optimal transport. *Advances in neural information processing systems*, 26:2292–2300, 2013.
- [9] M. Dellnitz and A. Hohmann. A subdivision algorithm for the computation of unstable manifolds and global attractors. *Numer. Math.*, 75(3):293–317, 1997.
- [10] M. Dellnitz and O. Junge. On the approximation of complicated dynamical behavior. *SIAM J. Numer. Anal.*, 36(2):491–515, 1999.
- [11] N. Dunford and J. T. Schwartz. *Linear operators. Part II*. Wiley Classics Library. John Wiley & Sons, Inc., New York, 1988. Spectral theory. Selfadjoint operators in Hilbert space, With the assistance of William G. Bade and Robert G. Bartle, Reprint of the 1963 original, A Wiley-Interscience Publication.
- [12] G. Froyland and M. Dellnitz. Detecting and locating near-optimal almost-invariant sets and cycles. *SIAM Journal on Scientific Computing*, 24(6):1839–1863, 2003.
- [13] A. Genevay, L. Chizat, F. Bach, M. Cuturi, and G. Peyré. Sample complexity of sinkhorn divergences. In K. Chaudhuri and M. Sugiyama, editors, *Proceedings of Machine Learning Research*, volume 89 of *Proceedings of Machine Learning Research*, pages 1574–1583, 2019.
- [14] C. S. Hsu. A generalized theory of cell-to-cell mapping for nonlinear dynamical systems. *Trans. ASME Ser. E. J. Appl. Mech.*, 48(3):634–642, 1981.
- [15] F. Y. Hunt. Unique ergodicity and the approximation of attractors and their invariant measures using Ulam’s method. *Nonlinearity*, 11(2):307–317, 1998.
- [16] S. Klus, A. Bittracher, I. Schuster, and C. Schütte. A kernel-based approach to molecular conformation analysis. *The Journal of chemical physics*, 149(24):244109, 2018.
- [17] S. Klus, P. Koltai, and C. Schütte. On the numerical approximation of the perron-frobenius and koopman operator. *Journal of Computational Dynamics*, 3(1):51, 2016.
- [18] P. Koltai, J. von Lindheim, S. Neumayer, and G. Steidl. Transfer operators from optimal transport plans for coherent set detection. *Physica D*, 426:132980, 2021.
- [19] E. N. Lorenz. Deterministic nonperiodic flow. *Journal of atmospheric sciences*, 20(2):130–141, 1963.
- [20] R. J. McCann. Polar factorization of maps on Riemannian manifolds. *Geom. Funct. Anal.*, 11(3):589–608, 2001.
- [21] G. Monge. Mémoire sur la théorie des déblais et des remblais. *Histoire de l’Académie royale des sciences avec les mémoires de mathématique et de physique tirés des registres de cette Académie*, pages 666–705, 1781.
- [22] J. Niles-Weed and P. Rigollet. Estimation of Wasserstein distances in the spiked transport model. arXiv:1909.07513, to appear in Bernoulli, 2019.
- [23] F. Nüske, H. Wu, J.-H. Prinz, C. Wehmeyer, C. Clementi, and F. Noé. Markov state models from short non-equilibrium simulations—analysis and correction of estimation bias. *The Journal of Chemical Physics*, 146(9):094104, 2017.
- [24] G. Peyré and M. Cuturi. Computational optimal transport. *Foundations and Trends in Machine Learning*, 11(5–6):355–607, 2019.
- [25] F. Santambrogio. *Optimal Transport for Applied Mathematicians*, volume 87 of *Progress in Nonlinear Differential Equations and Their Applications*. Birkhäuser Boston, 2015.
- [26] W. Tucker. The Lorenz attractor exists. *Comptes Rendus de l’Académie des Sciences-Series I-Mathematics*, 328(12):1197–1202, 1999.
- [27] S. M. Ulam. *A collection of mathematical problems*. Interscience Tracts in Pure and Applied Mathematics, no. 8. Interscience Publishers, New York-London, 1960.
- [28] C. Villani. *Optimal Transport: Old and New*, volume 338 of *Grundlehren der mathematischen Wissenschaften*. Springer, 2009.
- [29] C. Wehmeyer and F. Noé. Time-lagged autoencoders: Deep learning of slow collective variables for molecular kinetics. *The Journal of chemical physics*, 148(24):241703, 2018.
- [30] M. O. Williams, I. G. Kevrekidis, and C. W. Rowley. A data-driven approximation of the Koopman operator: Extending dynamic mode decomposition. *Journal of Nonlinear Science*, 25(6):1307–1346, 2015.

- [31] M. O. Williams, C. W. Rowley, and I. G. Kevrekidis. A kernel-based method for data-driven Koopman spectral analysis. *Journal of Computational Dynamics*, 2(2), 2015.